

Article

The Ballynoe Stratiform Barite Deposit, Silvermines, County Tipperary, Ireland

Colin J. Andrew

Independent Researcher, Touchstone, Ardracran, Navan, C15 E5A0 County Meath, Ireland; candrew@iol.ie;
Tel.: +353-87-241-2290

Abstract: The Ballynoe barite deposit is a conformable, mineralised horizon of Lower Carboniferous age overlying a diastem and mass faunal extinction demarking the transition from a quiet water environment to one of dynamic sedimentation. The geometry of the barite orebody correlates with the palaeotopography of the footwall, which acted as an important control over the lateral extent, thickness, and nature of the mineralisation. Sedimentary features within the barite horizon suggest that it was precipitated in the form of a cryptocrystalline mud which underwent major diagenetic modification resulting in extensive stylolite formation, recrystallisation, and remobilisation. There is abundant and compelling geological and isotopic evidence for early local exhalation from the presence of a hydrothermal vent fauna consisting of delicately pyritised worm tubes and haematized filaments of apparent microbial origin. The worm tubes are remarkably similar to examples from modern and ancient volcanic-hosted massive sulphide deposits, and the filamentous microfossils have similarities to modern Fe-oxidising bacteria. Strontium in the barite has an $^{87}\text{Sr}/^{86}\text{Sr}$ ratio indistinguishable from seawater between 350 and 344 Ma whilst oxygen isotopes from barite and chert suggest a diagenetic origin in equilibrium with such seawater around 60–70 °C. Fluid inclusion studies have shown that, in general, low temperature inclusions are very saline (20%–25%) whilst at higher homogenisation temperatures they are more dilute (9%–12%).

Keywords: stratiform; Lower Carboniferous; barite; Silvermines district; exhalation



Citation: Andrew, C.J. The Ballynoe Stratiform Barite Deposit, Silvermines, County Tipperary, Ireland. *Minerals* **2024**, *14*, 498. <https://doi.org/10.3390/min14050498>

Academic Editors: Norman Moles and Francisco J. González

Received: 23 February 2024

Revised: 30 April 2024

Accepted: 4 May 2024

Published: 9 May 2024



Copyright: © 2024 by the author. Licensee MDPI, Basel, Switzerland. This article is an open access article distributed under the terms and conditions of the Creative Commons Attribution (CC BY) license (<https://creativecommons.org/licenses/by/4.0/>).

1. Introduction

The carbonate-hosted Irish Midlands Orefield covering around 22,000 km² is ranked first in the world in terms of zinc metal discovered per sq. km, and second for lead [1,2] with in excess of 14 Mt of contained zinc metal found to date. The largest deposit at Navan exceeds 150 Mt of production and remaining resources, with four deposits (Tynagh, Silvermines, Lisheen, Galmoy) brought into production since 1962, and a further 20 prospects discovered to date. The orefield has also historically been a major producer of barite (an EU-designated critical raw material) and all of the deposits contain barite to some degree (see Appendix A).

The deposits in the Irish Midlands such as Navan, Tynagh, Silvermines, Lisheen, Galmoy, and Pallas Green and others that host this vast resource show varying host-rocks, mineral textures, and thermo-chemical and isotopic signatures that together neither equate to Sedex nor MVT types. However, amongst this apparent diversity lie some major similarities that form the basis of the definition of being “Irish-type” [1]. The Silvermines deposits together form the type-example of Irish-type Zn–Pb deposits illustrating the relationship between epigenetic ore zones (interpreted as feeders) and near-surface replacement stratiform sediment-hosted orebodies [1–3]. Whilst most Irish-type deposits around the world were typically formed syndiagenetically in the shallow subsurface, and exhalation is not a common attribute, in certain deposits in Ireland, definitive sea-floor deposition of sulphides and oxides (and thus by equivalence, barite) has been conclusively demonstrated at Tynagh [4], Crinkill [5], and Silvermines [6,7] and in the Conglomerate Group Ore at Navan [8,9].

The base-metal and barite deposits in the Silvermines area occur on the northern flank of the Silvermines Mountains, some 8 km south of the market town of Nenagh in north County Tipperary in the Irish Midlands. The earliest description of the deposits in the Silvermines area dates back to 1861 in the First Series sheet memoirs of the Geological Survey of Great Britain [10] whilst Griffith [11], Rhoden [12], Barrett [13], Taylor & Andrew [14], Taylor [15], Andrew [1,16], and Mullane & Kinnaird [17] have described the contemporary knowledge of the mineralisation in detail. Additional data on the deposits have been contributed by Greig et al. [18], Coomer & Robinson [19], Larter et al. [20], Bruck [21], and Boyce et al. [6,7]. However, these publications have largely focused on the base-metal mineralisation.

The Ballynoe barite deposit is a substantial part of the Silvermines mineralising system although literature is sparse on the barite ore zone itself, with only Barrett [13] and Mullane & Kinnaird [17] specifically describing its setting and features. The Silvermines orebodies consist of three contiguous stratiform zones, two of which (the Upper G and B-Zones) contained economic Zn–Pb–Ag grades hosted in massive pyrite, siderite, and barite whilst the third (the Ballynoe deposit) comprises massive barite with only traces of Zn–Pb. These mineralised zones totalling some 17.7 Mt @ 6.4% Zn, 2.5% Pb also contain 0.64 Mt of massive barite in addition to the 5.27 Mt of barite mined from the Ballynoe section. They are all developed at a single horizon and genetically may be considered as a single entity. Cross-cutting mineralisation of Zn–Pb–Fe sulphides and barite is seen at lower stratigraphic levels and may be logically assumed to represent conduits to the stratiform ore horizon.

This paper reviews existing published data on the Silvermines system, focusing on the Ballynoe barite zone, and attempts to draw together some of the available information from a number of unpublished sources including PhD theses, mine records, and company reports to present a coherent account of the formation of the barite deposit.

2. History

The discovery of barite at Ballynoe must be credited to the Geological Survey of Great Britain, which mapped the area between 1856 and 1860. In 1956 the Silvermines Lead and Zinc Company Limited commenced quarrying the barite at the outcrop and shipped 3800 tonnes at 80% BaSO₄ to England. In the following year the company commenced drilling the deposit with the hope of locating base-metal mineralisation associated with the barite, completing 23 holes with little base-metal but defining a substantial deposit of barite. In May 1959 the Magnet Cove Barite company (“Magcobar”) took out a lease over the property and extended the drilling to eventually define over 5 Mt of barite at an average grade of 85% BaSO₄ [22].

In October 1962 the Canadian company International Mogul Mines also concluded a farm-in agreement with the Silvermines Lead & Zinc Company to explore an 80 km² area at Silvermines. Drilling commenced in June 1963 and by December 1964 almost 10 Mt of economic zinc-lead ore had been defined. Underground mining operations commenced in 1968 until closure in July 1982, having milled 11.86 Mt of ore grading 2.83% Pb and 7.35% Zn from underground workings on a number of orebodies, of which the B and G zones, located at the same stratigraphic horizon and part of the same orebody as the Ballynoe barite, were economically the most substantial.

Magcobar Ireland Limited (latterly Dresser Minerals International Inc) mined 5.27 Mt barite (~90% BaSO₄) from the Ballynoe open pit (Figures 1 and 2) (and latterly 188,700 tonnes from underground workings) between 1963 and mine closure in April 1993 [2,22] (Figures 1–3). To access this ore, around 8.5 to 9 Mt of overburden and waste rock were stripped and largely dumped above the open pit. These dumps have recently been landscaped and revegetated whilst the pit is now completely flooded.

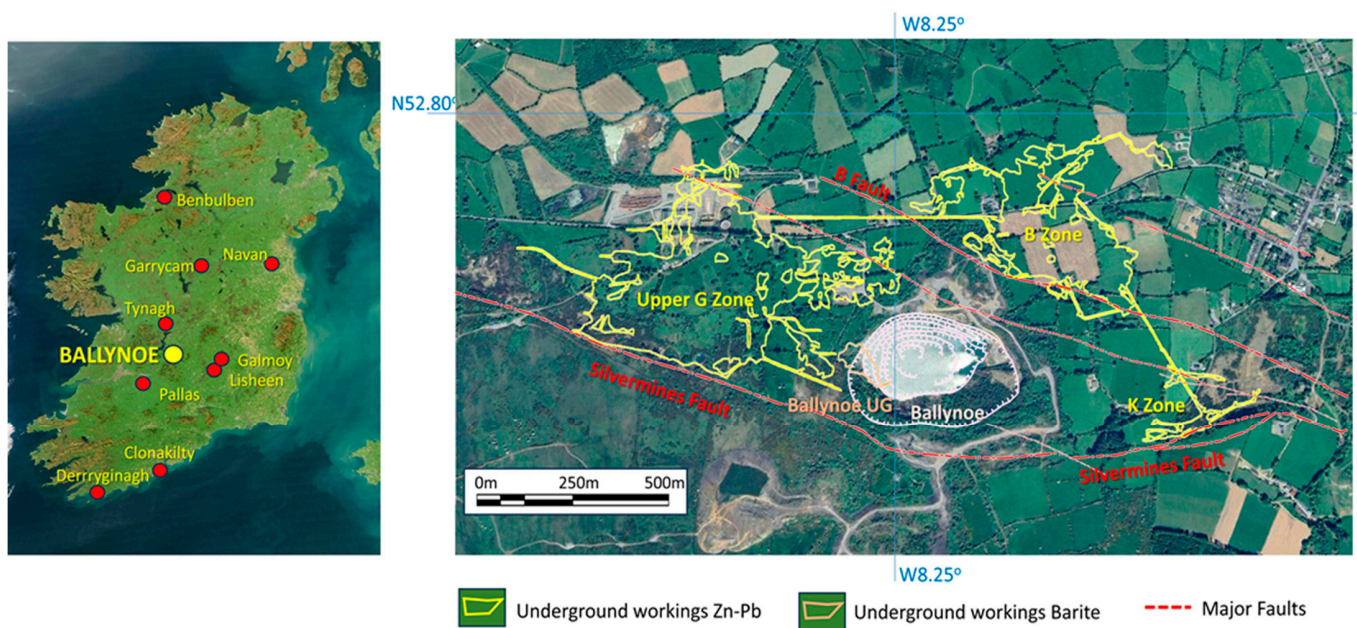


Figure 1. Location map of Ballynoe in central Ireland showing other barite occurrences; and (right) satellite image of the Silvermines District showing the underground workings of the Mogul Mine and the open pit and underground workings at Ballynoe.

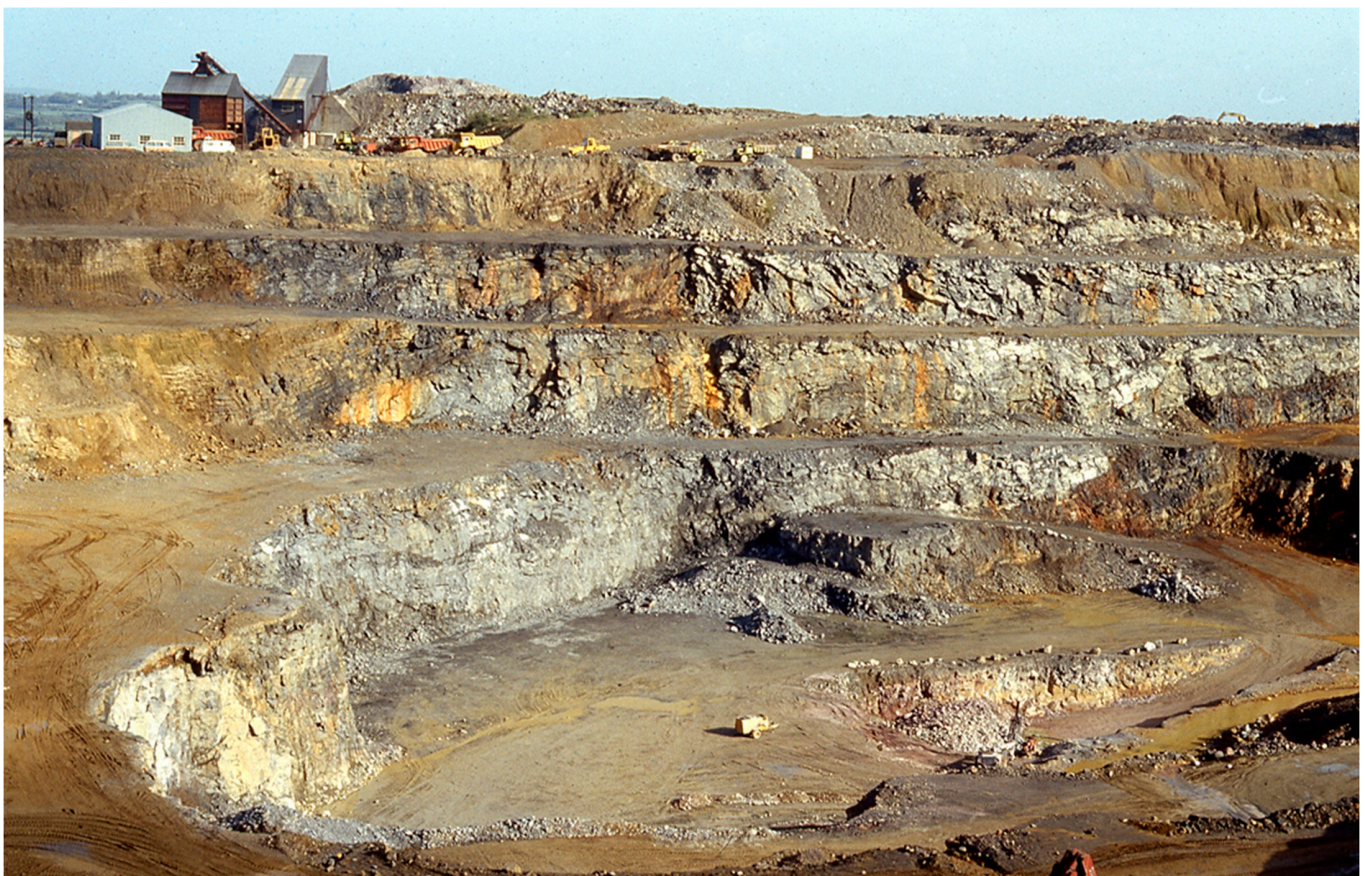


Figure 2. General view of the Ballynoe pit (Magcobar) facing to the NNE, with pit bottom on Bench 5 in July 1986. Bench height varies between 10 and 12 m.

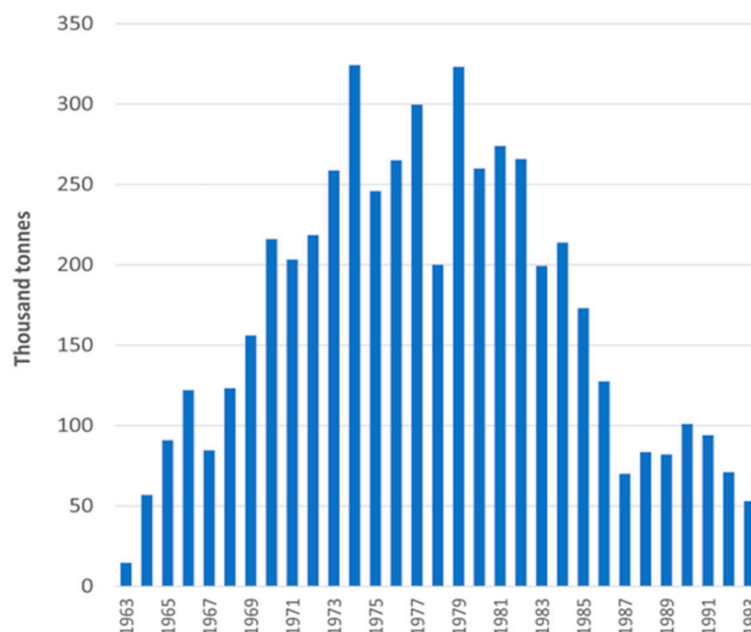


Figure 3. Production of lump grade (>85% BaSO₄) from the Ballynoe Mine between 1963 and closure in 1993. Production data from Company Records.

3. Geological Setting

The stratigraphy of the Silvermines District has been described by Taylor and Andrew [14], Taylor [15], and Andrew [16] and its regional setting by Brück [21] and Philcox [23]. In simple terms, the local Silurian greywacke basement is overlain by a sequence of red, green, and white siliciclastics of the Hastarian age, which pass conformably up into a marginal marine transgressive sequence of, initially, silty mudrocks passing upwards into a sequence of oolitic and argillaceous bioclastic limestones (the Ballysteen Formation) before seeing the development of the regionally extensive Waulsortian mudbank limestone comprising pale grey stromatactid biomicrites and its equivalents [24–26]. Depositional patterns and thicknesses were strongly influenced by the development of basal areas, which generally follow earlier ENE and NE’erly Caledonian structural trends in the pre-Carboniferous basement, which have been described in detail [1,23,27–30].

In the Silvermines District, a sharp formational boundary at the top of the argillaceous limestones of the Ballysteen Formation is defined by mass extinction of fauna and by a thin (0.05–1.0 m) distinctive greenish argillite (“the Green Shale”) which may have a tuffaceous component as seen at Lisheen and Pallas Green where it has been dated at between 350.5 and 348.2 Ma [31].

Above the Green Shale at Silvermines, the Waulsortian equivalent marks the transition from a quiet water environment to one of dynamic sedimentation and comprises a sequence of complex limestone and dolomite breccias that most authors familiar with Silvermines consider to be chaotic debris flows, focussed down the palaeoslope from the points of maximum throw on the ore controlling fault system (Figures 4–6).

The principal structural setting comprises a WNW-trending, NNE-dipping array of left-stepping fault segments with maximum displacements of between 130 and 375 m, linked by relay ramps and generally referred to as the Silvermines Fault Zone [32] (Figure 6).

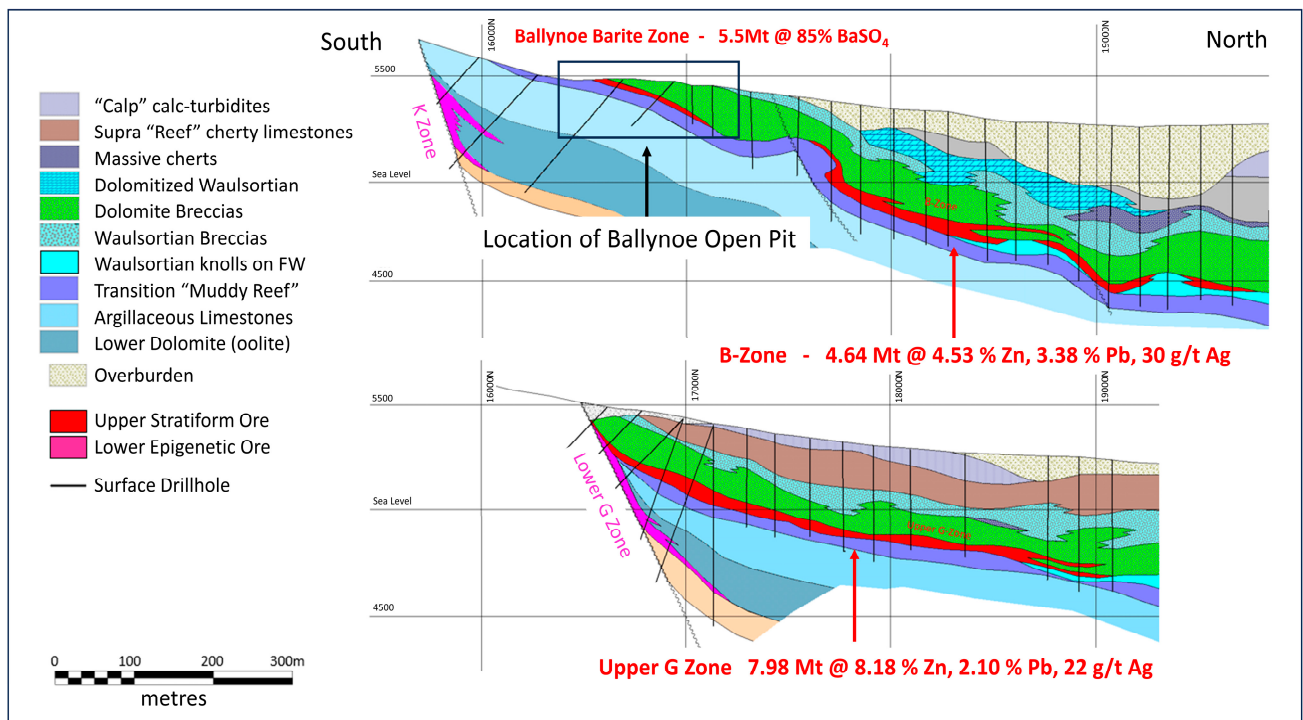


Figure 4. N–S Sections through the Silvermines orebodies. Redrawn from [14].

See Figures 6 and 7 for details of the Ballynoe barite zone part of the stratiform orebody.

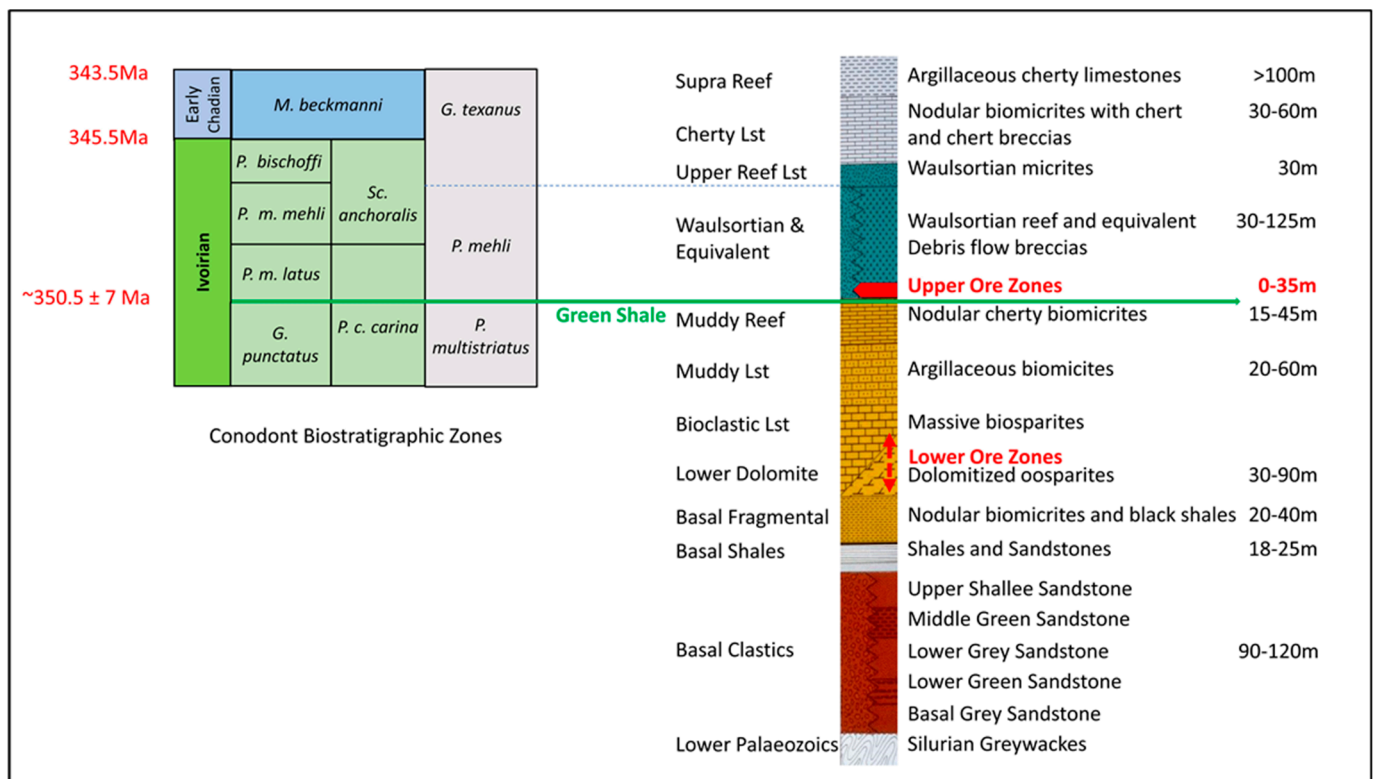


Figure 5. Stratigraphic column for the Silvermines and Ballynoe area.

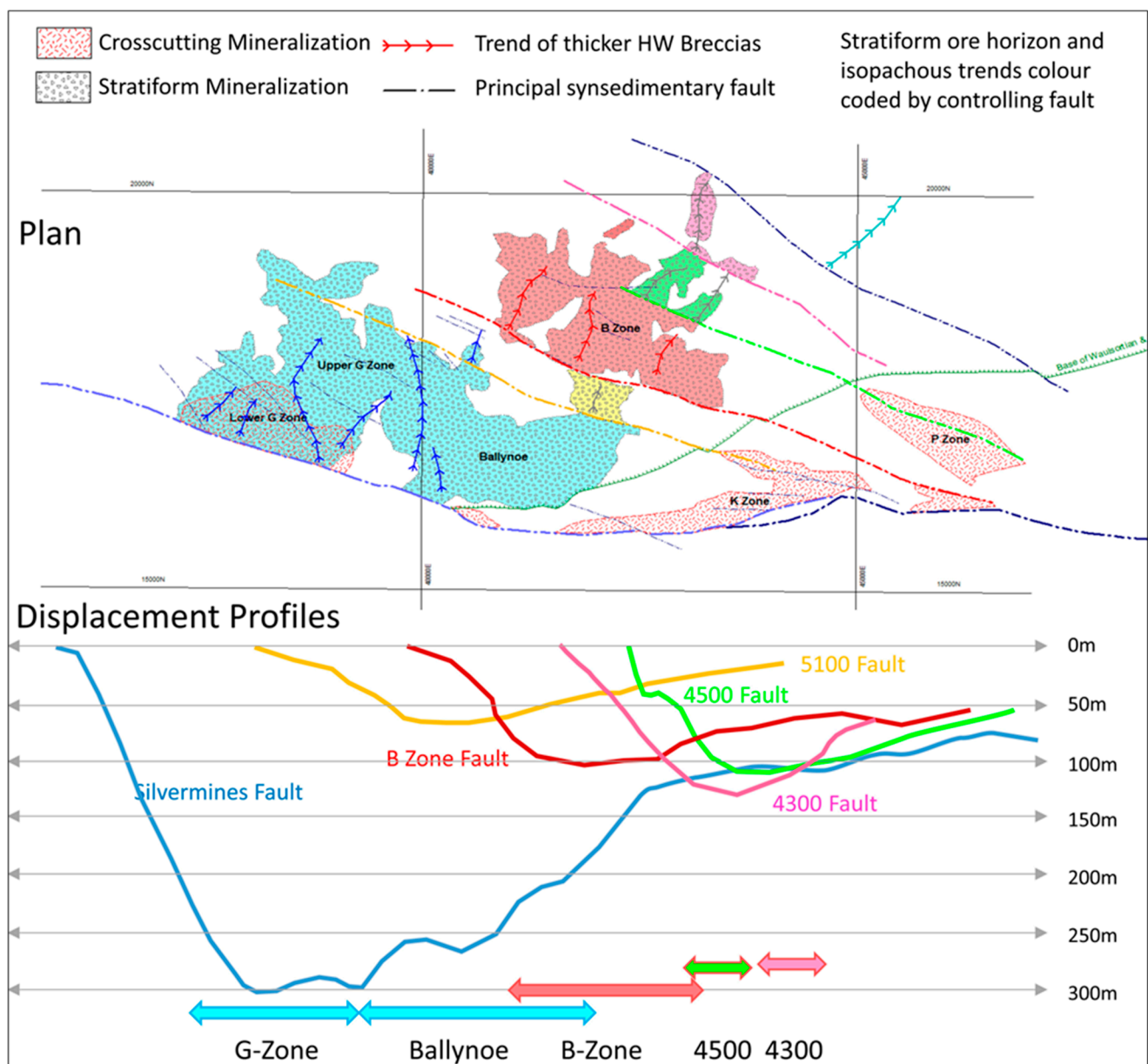


Figure 6. Plan of the stratiform orebodies, colour coded to the controlling principal structures of the Silvermines fault complex. Displacement profiles shown across the individual branches of the fault complex. The plan also shows the principal trends of the thickened hangingwall breccias.

4. Setting of the Barite Orebody

Immediately underlying the strongest base-metal and barite mineralisation at Silvermines, the Muddy Reef Limestone is extensively replaced by chert in the uppermost part of the succession, and black chert lenses up to 5 m thick are of common occurrence below the barite horizon. A similar thickness of chert is reported underlying the ‘Upper G Zone’ orebody [33].

The Muddy Reef Limestone is generally capped by an irregular development of green argillite, the “Green Shale” of previous authors [2,8–10], which also interdigitates with the barite horizon. The thickest development of this shale is found to occur in minor surface depressions at the top of the Muddy Reef Limestone, ranging from a few cm up to a maximum of around 1.2 m. Slump structures are evident in the thicker shale lenses and rare, angular micro-fragments of bioclastic limestone are sometimes incorporated into the slumped argillite. Barrett [13] noted that based on its constituent mineralogy the green

argillite may be divided into two facies: (a) a chlorite–illite–quartz shale \pm barite, and (b) a siderite–chlorite–illite–quartz shale.

Type (a) has the most widespread distribution in the vicinity of the barite zone and also comprises numerous shale intercalations within the basal part of the barite orebody indicative of density differential slumping.

Type (b) is defined by its siderite (FeCO_3) content and is a paler shade of green than type (a). It is generally less laminated and not greatly affected by slumping. Type (b) is preferentially developed underlying the siderite ore host lithologies in the B-Zone and the barren siderite developed to the north of the Ballynoe barite body.

The Ballynoe barite deposit is a complex interstratification of sulphate, sulphide, oxide, silicate, and carbonate minerals. The mineralised horizon exhibits both lateral and vertical zonation which is of considerable genetic importance. The barite horizon is conformable with the top of the Muddy Reef Limestone, and in both strike and dip the orebody is lenticular in shape, with ore-grade barite quickly pinching out into low-grade material towards the margin of the lens. Economic barite mineralisation extends for approximately 700 m along the strike and for 400 m down-dip from the outcrop. The average thickness of the orebody is around 10 m of massive barite, with a maximum thickness of close to 20 m being developed in the west–central part of the deposit (Figures 7–12). The location, disposition, and thickness of the barite body shows an intimate relationship to the topography of the footwall contact as described by previous authors [13–16,33].

Lying at the same horizon and partially connected to the west of the barite zone, the stratiform Upper-G orebody occurs as massive, partly brecciated pyrite at the base of a thick sequence of dolomite breccias, and immediately overlies the Footwall Mudbank Reef Limestone (Figures 4, 7 and 8). The maximum thickness of economic ore (30 m) is attained in the southern portion of the orebody near the northwest-trending faults that define its southern limit. The southwestern and southeastern boundaries, which closely follow the limits of massive pyrite development, are straight and well defined, whereas the northern limits are irregular and reflect the uneven development of the Footwall Mudbank Limestone against which the pyritic ore pinches out. The orebody base is in general lithologically sharp, being demarked by the abrupt change from massive pyrite to footwall sediments almost devoid of sulphides, but occasionally the sediments, with progressive increase in pyrite content, grade into the massive pyrite. The upper contact is, in contrast, always lithologically well defined: it is indicated by the change from massive pyrite to dolomite breccia or to thin shale bands overlain by dolomite breccias. Pyrite and marcasite, which constitute 75% of the sulphide content, sphalerite (20%), and galena (4%) are the dominant sulphides; trace quantities of chalcopyrite, tennantite, boulangerite, marcasite, bournonite, jordanite, and pyrrotite occur. Of the gangue minerals, dolomite, chert, clay minerals, calcite, barite, and quartz are present in descending order of abundance.

Also contiguous to the NE of the Ballynoe barite zone, part of the B-Zone orebody is dominated by pale buff to pink brecciated fine-grained barite that contains distinctive inclusions of haematite and jasperoid at its base. The characteristic mineralisation is of fine intraclastic disseminations of galena and pyrite with minor fine-grained sphalerite. The pyrite zone comprises massive or brecciated pyrite, which is either finely crystalline or colloform, and displays a variety of structures including spheroids, concentric bands, plumose bodies, and framboids. It typically contains extremely fine-grained sphalerite and galena, as both disseminations and coarser replacements. Locally, the pyrite is in the form of a tightly packed, poorly sorted breccia in an argillaceous or dolomitic matrix, partly replaced by fine-grained sphalerite and galena. The siderite zone is characterised by a breccia of clasts of line-grained buff to grey siderite, of varied size, angularity, and degree of packing, which appear locally stratified with interbeds of undisturbed shale. In parts of the B-Zone, economic sphalerite dominated base-metal mineralisation occurs as intraclastic disseminations and veinlets.

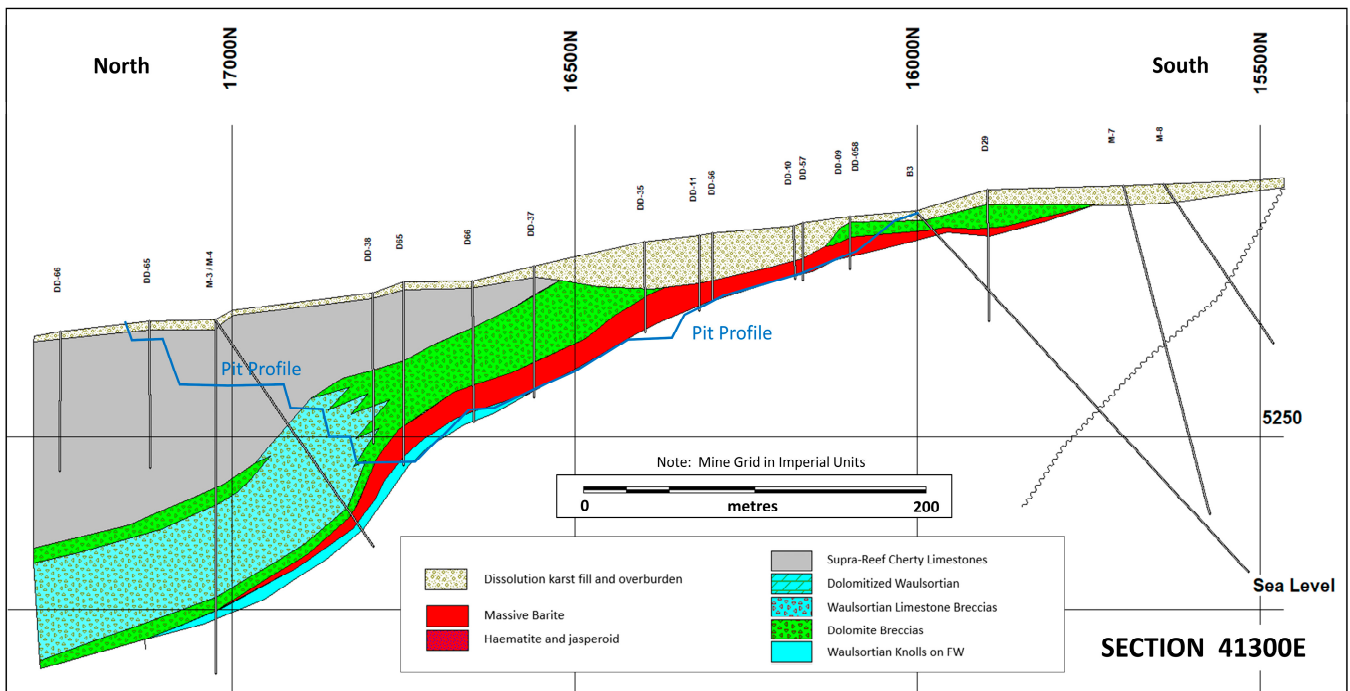


Figure 7. North–South Section 41300 E through the Ballynoe Barite Zone and open pit.

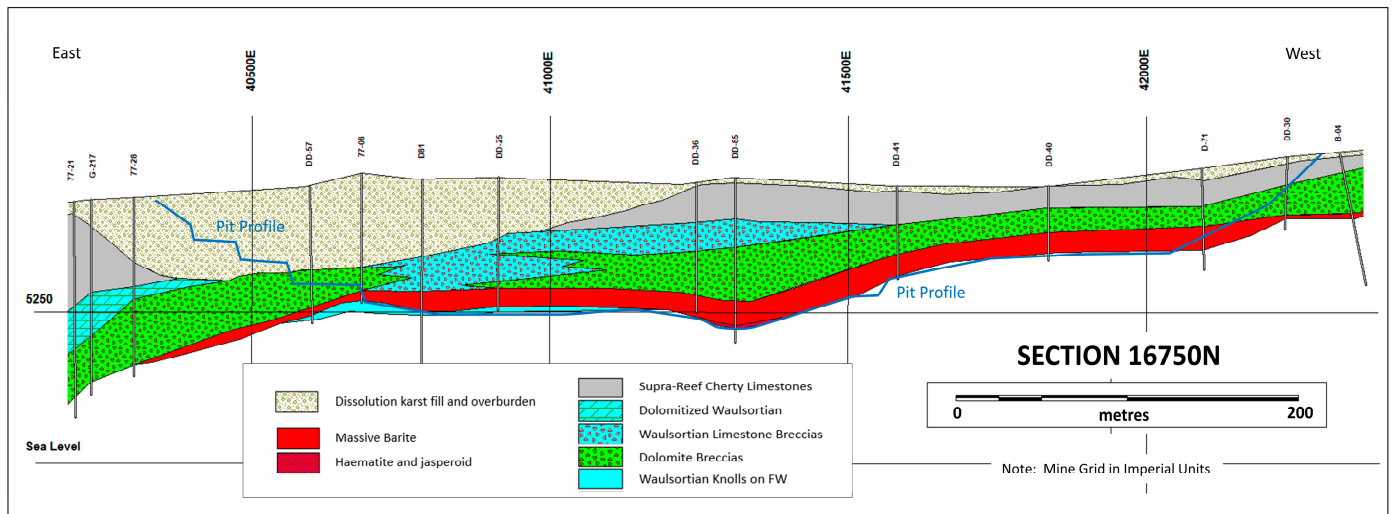


Figure 8. East–West Section 16,750 N through the Ballynoe Barite Zone and open pit.

The geometry of the barite, siderite, and pyrite orebody host lithologies correlates with the palaeotopography of the footwall, with the topography acting as an important control over the lateral extent, thickness, and nature of the mineralisation which thins over Waulsortian footwall knolls and thickens in troughs between such knolls. Connolly-type plots of the distance above an arbitrary plane of the Green Shale footwall shown in Figures 9 and 10 reveal a spectacular correlation between the troughs and the extent of the mineralisation, strongly suggestive of a sedimentary environment control.

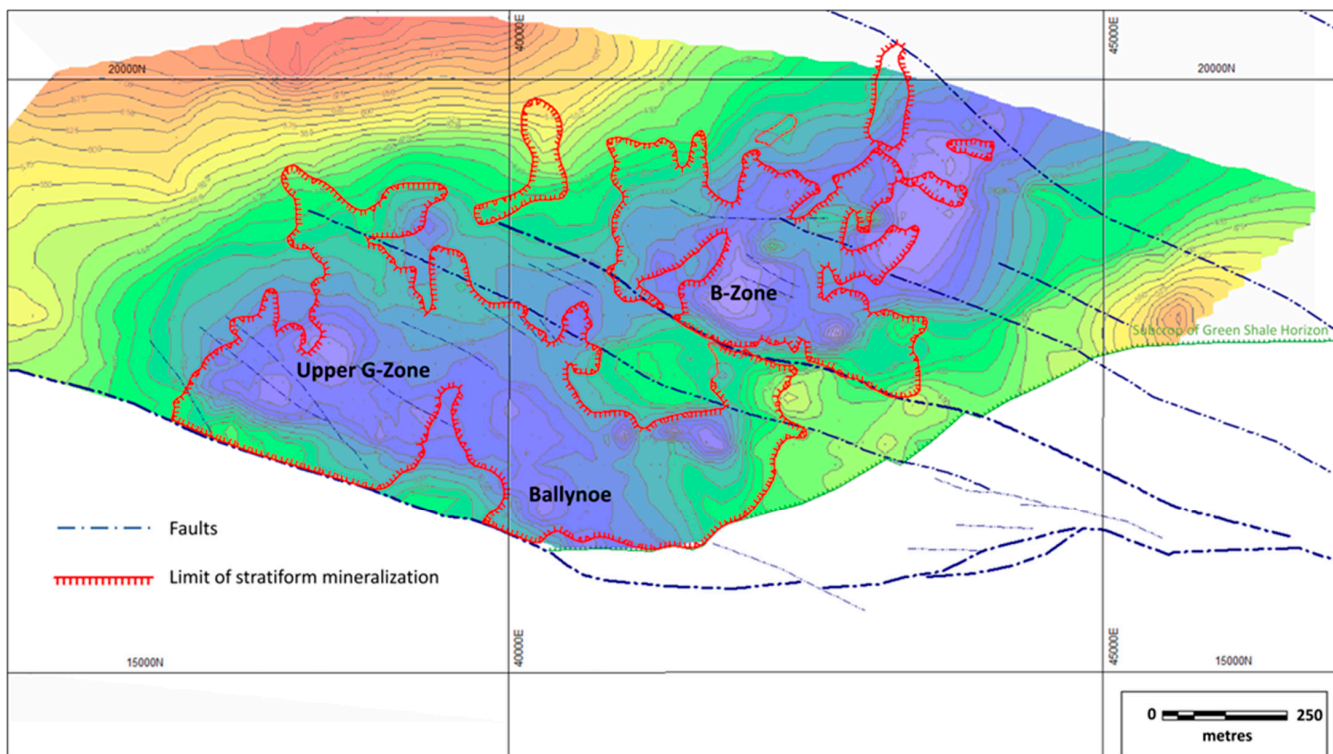


Figure 9. Connolly-type plan of the distance above a uniformly dipping plane, of the footwall contact of the mineralised horizon (the Green Shale) showing the troughs (blues) and highs (reds). The plan also shows the extent of the stratiform mineralised horizon and principal structures of the Silvermines Fault zone.

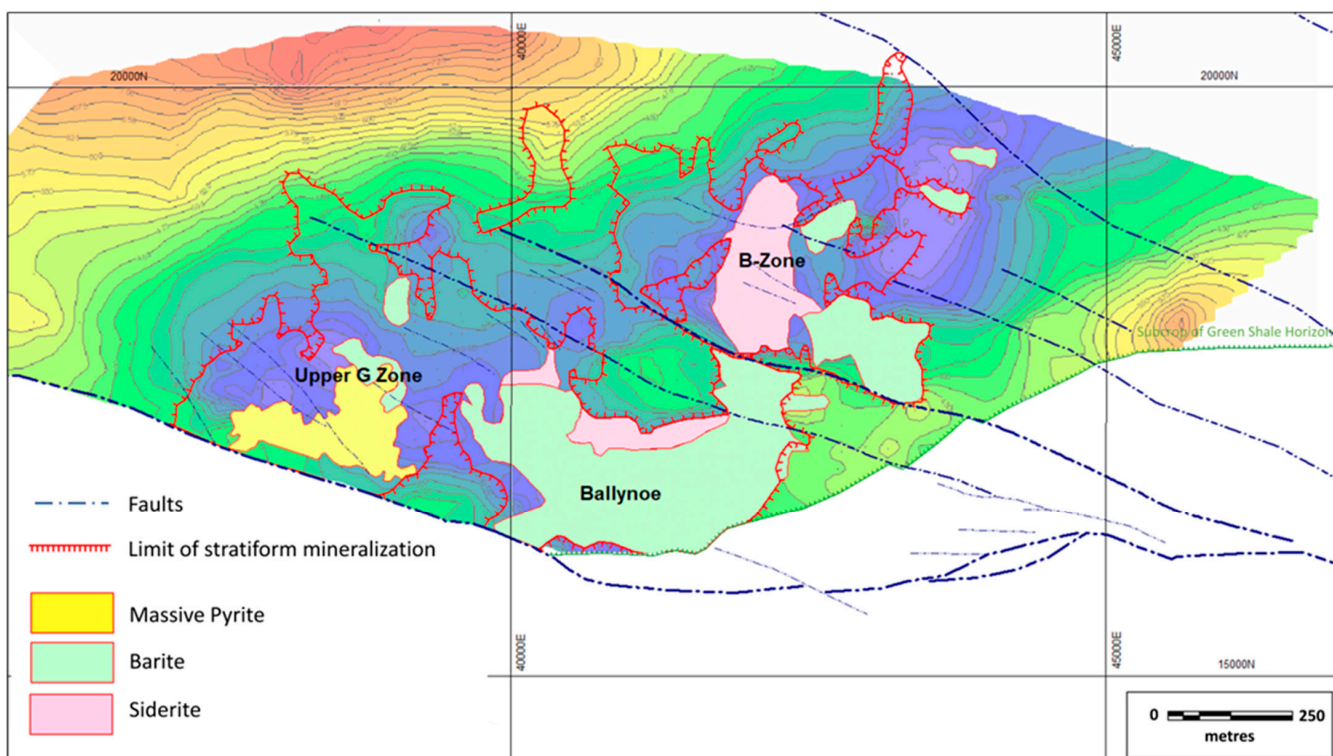


Figure 10. Similar Connolly plot as in Figure 9 but also showing the extent of the primary stratiform orebody host lithologies.

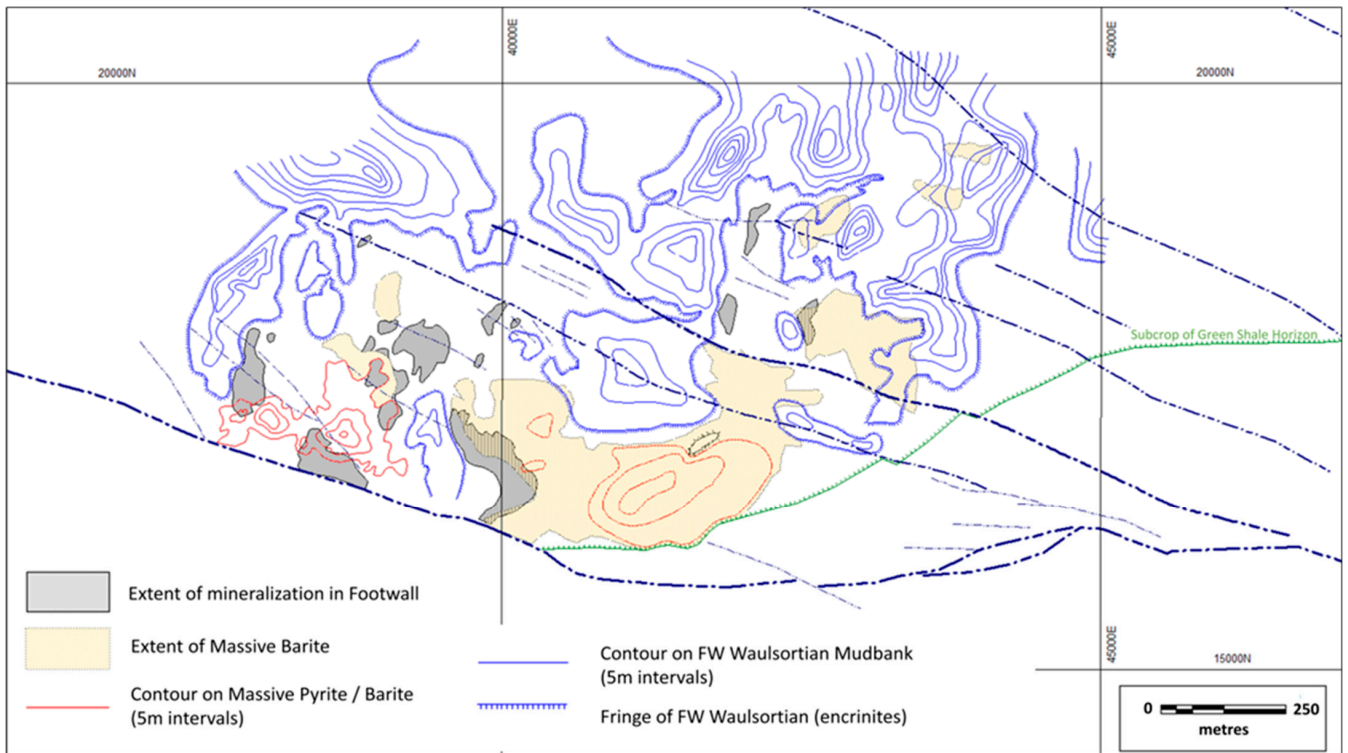


Figure 11. Plan to show the extent of chertification and mineralisation in the uppermost beds of the footwall Muddy Reef Limestones, the extent of the massive barite orebody with isopachs, and the development of the thickness and extent of the knolls of Waulsortian on the immediate footwall of the stratiform horizon.

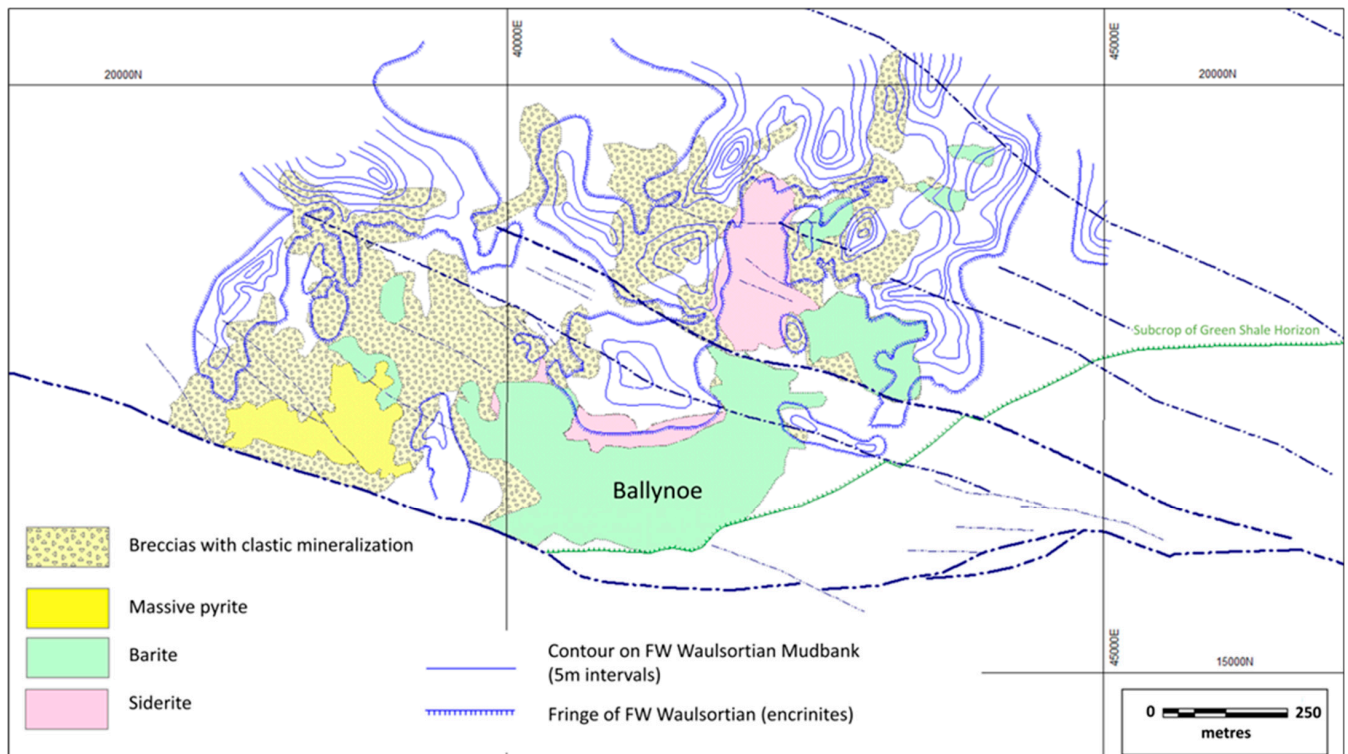


Figure 12. Similar plan to Figure 11 but showing the extent of the primary stratiform orebody host lithologies and the extent of the control of its distribution by knolls of Waulsortian on the immediate footwall to the stratiform horizon.

5. Geology of the Barite Orebody

Barrett [13] and Mullane & Kinnaird [17] defined a number of distinct stratigraphic units within the barite on the basis of differences in mineralogy texture and sedimentological features (Figure 13). However, these divisions are extremely variable in extent, and often co-exist.

The basal Unit 1, typically 1–2 m in thickness, can be sub-divided into the following types: (1a) barite breccia; (1b) banded haematite–barite with massive jasper; (1c) replacement of the footwall by barite and pyrite.

The development of barite breccia (Unit 1a) is associated with local changes of slope in the footwall, and its formation is best developed on the flanks of the ‘eastern dome’. On the north-western flank of this footwall ‘high’, lensoid masses of siliceous, crinoidal debris are overlain by pyritic, green argillites overlain by a thin, baritic breccia sequence (Figures 13, 14a and 15a). The barite breccia consists of scattered clasts of brick-red to pink barite set in a matrix of highly-slumped, green argillite. Fragments of bioclastic limestone are not infrequent in the breccia. The barite breccia clasts may be angular, rounded, or diffuse. The diffuse barite occurs in zones of intense slumping and is often sheared and invaded by slivers of green argillite parallel to the plane of movement. The slumped material has been subjected to secondary silicification and pyritisation. The fact that the barite breccia is confined to the flanks of the ‘eastern dome’ suggests gravitational slumping and the existence of the topographical high during early barite deposition. This barite breccia sequence rarely exceeds 0.5 m in thickness in Ballynoe whilst a zone of thick barite breccia is developed in a ‘low’ situated in the south-east of the B Zone orebody (Figures 11 and 12). The brecciated sequence is up to 8.5 m thick and consists of sub-angular clasts of micro-crystalline, brown barite, set in a base-metal sulphide-rich muddy carbonate matrix.

The banded haematite–barite with jasper (Unit 1b) is quite complex, both mineralogically and texturally, comprising quartz (as inclusion-rich equant crystals in jasperoid and as clear fracture-filling material), blood-red haematite (as the inclusions in jasperoid), sphalerite, pyrite, galena, boulangerite, barite, and minor calcite [34].

Lithology	Average Thickness	Density
 Dolomite Breccias - hangingwall sequence		
Unit 7 - Patchy replacement of dolomite breccias by late crystalline barite	1.5m	4.0
Unit 6 - Massive colloform sulphides	1.0m	
Unit 5 - White fine grained crystalline “cap” barite	1.5m	4.5
Unit 4 - Black to dark grey microcrystalline barite	9.0m	4.3
Unit 3 - Augen or spherulitic mottled barite	1.5m	4.2
Unit 2 - Siliceous augen and jasperoidal haematitic barite	3.0m	4.1
Unit 1 - Barite breccias, banded jaspers and dark red haematitic barite	1.0m	3.8
Green argillite	0.2m	
Muddy Reef - footwall sequence		

Figure 13. Sketch diagram showing the various units of the barite orebody as defined on the basis of differences in mineralogy texture and sedimentological features. Data from [13,17].

The banded haematite unit is a conformable, ironstone horizon, and is analogous to the Tynagh bedded ironstone formation [35], although developed on a very much smaller scale. The bedded haematite at Ballynoe is unique to the barite deposit, and no comparable formations are reported from the ‘Upper G’ or ‘B’ zones. The haematite horizon averages 0.6 m in thickness and is best developed under the southern half of the barite body, pinching out entirely down-dip to the north. The horizon consists of lenses of massive haematite (up to 0.3 m thick) in a matrix of haematitic-barite and interlayered with goethite and jasper. Rare magnetite has been identified from crushed samples of massive haematite. Evidence such as graded particulate sediments and soft sediment slump fabrics suggests that the haematite was laid down as a sediment in a dynamic environment. Catlin [36] and Locklin [34] found no evidence that the jasperoid replaced an earlier-formed carbonate rock and concluded that it had formed as a sea-floor precipitate. Soft-sediment slumping and penecontemporaneous micro-faulting occur frequently throughout the horizon, and the carbonates are often pseudomorphically replaced by fine-grained aggregates of euhedral and subhedral pyrite.

Wherever the haematite horizon is underlain by green argillite, the sequence is balled-up and highly brecciated. It is possible that the upper surface of the Green Shale acted as a plane of decollement to the overlying haematite formation and initiated the slumping (Figure 14d).

A massive micritic carbonate mudbank is present in the northwest corner of the Ballynoe pit, and the barite ore body abuts this mudbank along its northern margin, indicating that the mudbank was present prior to mineralisation.

The gradual transition from ‘bedded ironstone’ into siliceous, iron-rich barite is marked by streaks and lenses of brilliant-red jasper (Figures 14a and 15a). Two types of jasper have been identified and possibly represent different generations. A colloform variety is associated with haematitic barite whilst a second variety replaces pyrite euhedra.

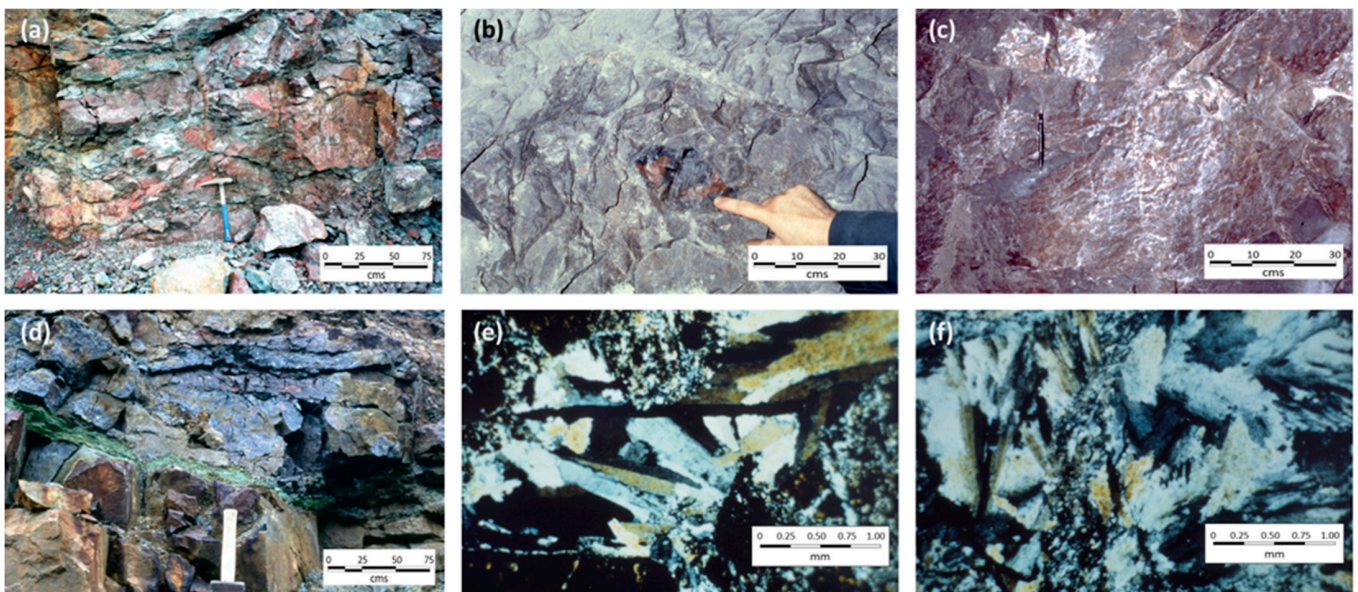


Figure 14. (a) Haematitic/jasperoidal barite, Ballynoe pit, south-west face Bench 6. (b) Clast of jasperoid set in massive grey-brown barite; ‘B-Zone’ 4937 Room. (c) Massive brown and white mottled barite with “zebra-type” lamination parallel to bedding; ‘B-Zone’ 4939 Room. (d) Distinctive Green Shale marker at top of Muddy Reef immediately underlying massive barite, Ballynoe Pit Bench 4 (e) Barite (white to grey to yellow) filling voids in fractured and brecciated jasperoid (dark brown to black). ‘B-Zone’ 49 area. Transmitted light with crossed polars; [36]. (f) Massive barite (white to grey to yellow) with minor opaque iron sulphides. ‘B-Zone’ 49 area. Transmitted light with crossed polars [36].

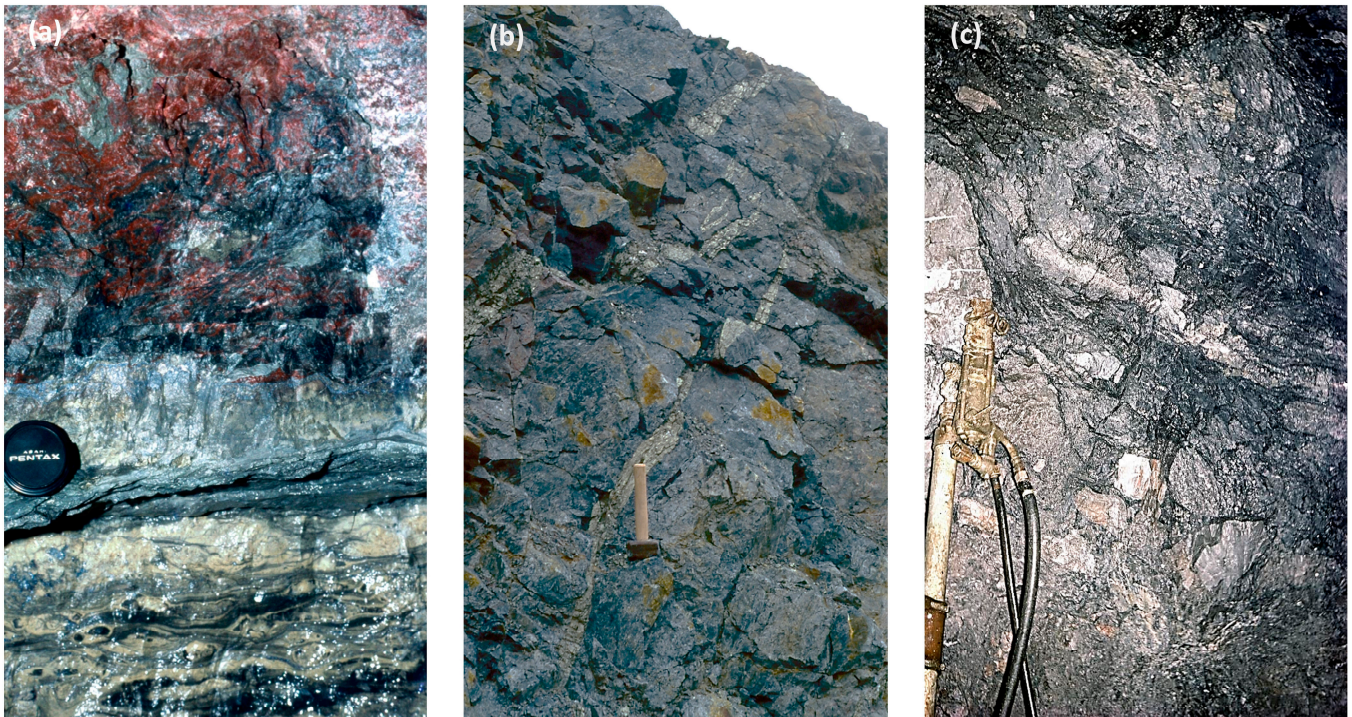


Figure 15. (a) Footwall contact of the haematitic massive barite sitting on 3–4 cm of the Green Argillite overlying strongly silicified and well mineralised (pale yellow sphalerite) Muddy Reef Limestone. Upper G Zone, East Panel, 2 Level. (b) Crustiform collomorph marcasite veins cutting massive grey barite. Ballynoe open pit. (c) Slumped debris flow of polymictic blocks set in argillaceous carbonate matrix; Two angular clasts of white and pink barite mid-lower centre. Jackleg drill for scale. B-Zone, 4510 Stope.

Colloform jasper is composed of coalescing spherulites about 100 microns in diameter which enclose amorphous, vuggy jasper often infilled by late crystalline white barite. A feature common to colloform jasper and not the replacement variety is dehydration (syneresis) cracks also often infilled with white barite. The cracks, which are wedge shaped, pinch out towards the centre of the jasper lens, diagnostic of the texture when dehydration of a silica gel takes place [37,38].

The morphology of the barite which replaces the footwall rocks (Unit 1c) is very distinctive and is easily differentiated from the allothigenic barite found in the basal green argillite sequence. This barite normally occurs as displacive growth stellate crystal groups and is always white to translucent in colour. Although the stellate barite crystals are developed in a very siliceous environment up to 3 m below the footwall contact with the principal mineralised horizon, the barite crystals are free from any silicification, suggesting emplacement post-dating the chertification of the Muddy Reef Limestone.

Two important periods of brecciation can be discerned with early-formed, haematite-bearing jasperoid being brecciated and then recemented by clear silica and minor pyrite. This material was in turn brecciated and recemented by barite, pyrite, and base-metal sulphides (with pyrite earliest), and minor calcite. The second brecciation/re-cementation event was accompanied by a “bleaching out” of the haematite on the edges of jasperoid clasts, giving a greenish-tan colour rather than a blood-red colour to the edges of the jasperoid clasts (Figure 14b).

The gradual transition from bedded ironstone into around 3 m of siliceous, jasperoidal haematitic barite of Unit 2 is marked by streaks and lenses of brilliant-red jasper (Figure 15a). The high silica content of the basal barite is not only due to jasper, which is normally restricted to areas of haematitic barite, but primarily due to the extensive replacement of barite by up to 10% of free silica. The pattern of this replacement is controlled by the

crystalline fabric of the barite and as a result a tabular meshwork of barite and quartz is often developed. Unit 2 passes gradually into Unit 3 which is dominated by “augen” or spherulitic mottled barite up to 1.5 m thick.

In Unit 3, layers of spherulitic and coarsely-crystalline, nodular barite are associated with the zones of stylolitisation and aggregations of spherulites around 0.02–0.05 m in diameter which form thin, colloform layers of red to pink barite conformable with the bedding and may be followed along strike for tens of metres. Stylolitic and spherulitic barite is confined in development to the central and thickest section of the orebody, this zone being very poorly defined in the east where the barite thins rapidly over the ‘eastern dome’. An empirical relationship is observed between the formation of stylolites and the occurrence of spherulitic textures in the barite.

Unit 4 volumetrically comprises perhaps 65% of the orebody and consists of well-bedded, grey to black microcrystalline barite with a uniform texture. In appearance, specimens resemble either dark anhydrite or a bituminous limestone. Microscopically, the fabric of the massive grey-black barite consists either of a compact aggregate of randomly orientated microplumose crystals or looser aggregates of microspherulites up to 0.5 mm in diameter which probably represent the primary crystalline state of the barite, a stage which is often obscured by subsequent diagenetic recrystallisation.

The microcrystalline grey-black barite of Unit 4 is rarely in direct contact with the hangingwall dolomite breccias and is normally overlain by a sequence of white barite (Unit 5) or massive pyrite (Unit 6) carrying disseminated galena and sphalerite up to 1 m in thickness, which is best developed over the western end of the Ballynoe barite orebody. This sulphide horizon attains its maximum thickness in troughs controlled by the uneven undulating upper contact of the barite with thinner development of pyrite overlying the crests of the undulations and carries less galena/sphalerite.

Zones of extensive stylolitisation in the fine-grained grey-black barite of Unit 4 tend to be overlain by layers of coarse, spherulitic barite crystals, the spherules often being pink to dark red in colour due to tiny inclusions of haematite. Horizontal-simple stylolites tend to be independent of the original barite fabric which is truncated randomly. The highly carbonaceous composition of the stylolites possibly represent the insoluble residue left from precipitation of the original barite. Such stylolites are considered to have formed early and at shallow depths [36]. In contrast to the simple stylolites, the horizontal-sutured variety are narrower in width, display a greater amplitude, and tend to be localised along the margins of megacrystalline barite ‘fans’.

Three facies of macrocrystalline barite in Unit 5 were recognised by Barrett [13]:

- (5a) barite conformable with the stratification and capping the orebody barite;
- (5b) irregular patches of white barite replacing the black, microcrystalline barite within the orebody;
- (5c) extensive hangingwall replacement by the white barite.

The macrocrystalline (type 5a) barite is hereafter described as the ‘cap’ barite. This is pure white in colour and is composed of coarse aggregates of macroplumose crystals up to 0.1 m in length. The horizon varies up to 1 m in thickness and was originally best developed near the present-day surface over the ‘eastern dome’. Masses of collomorphic pyrite are not uncommon within the basal development of the ‘cap’ barite (Figure 15b).

Associated with the development of secondary barite are crosscutting veinlets of thin barite (2–3 cm wide) which extend across the orebody from footwall to hangingwall, a vertical distance of more than 10 m. The veinlets trend NE–SW (the dominant joint trend) and invariably dip to the east at between 70–85°. This vein barite carries no sulphides.

The Ballynoe barite deposit exhibits a complex interstratification with the development of both lateral and vertical zonation. As such, the zonal divisions within the barite horizon can be extremely variable in extent, and often co-exist. For example, layers of spherulitic barite (Unit 3 type) may be developed throughout the black, microcrystalline barite of Unit 4. The white, crystalline barite of Unit 5 may be found as disseminations within Units 4

and 6. Units 2 to 4 carry ore-grade barite and constituted around 85% of the total tonnage mined.

Synsedimentary slumping is well developed throughout the barite ore body, particularly in Units 4 and 5. It is most obvious when the barite is of different colours and when it is intercalated with pyrite, as in Unit 4. Debris-flow clasts of red silicified barite and jasperoidal haematite are present in the lowest parts of the barite body (Figures 14a and 15a) [2,13–17,39]. They vary from angular to sub-rounded and have sharp margins. These originated as rip-up clasts from the erosion of the underlying unit. Another example of rip-up clasts, emphasised through colour contrasts, occurs close to the contact between barite Units 3 and 4. Angular clasts of Unit 3 (black) are incorporated at the base of Unit 4 (fawn-brown). The upper surface of Unit 3 is also scoured.

5.1. Geochemistry

At Ballynoe, the silica content of the immediate footwall to the barite body attains levels of up to 60% and then diminishes upwards through the barite orebody from 10% near the base in Units 1 and 2 to less than a few hundred ppm in Unit 4 (Figure 16) [13]. This silica within the barite is amorphous and cryptocrystalline and often associated with haematite as jasperoid in the lowermost parts of the orezone. As at Tynagh the iron-silica zone infills a palaeotopographic low or sag on the downthrown side of the fault complex [35].

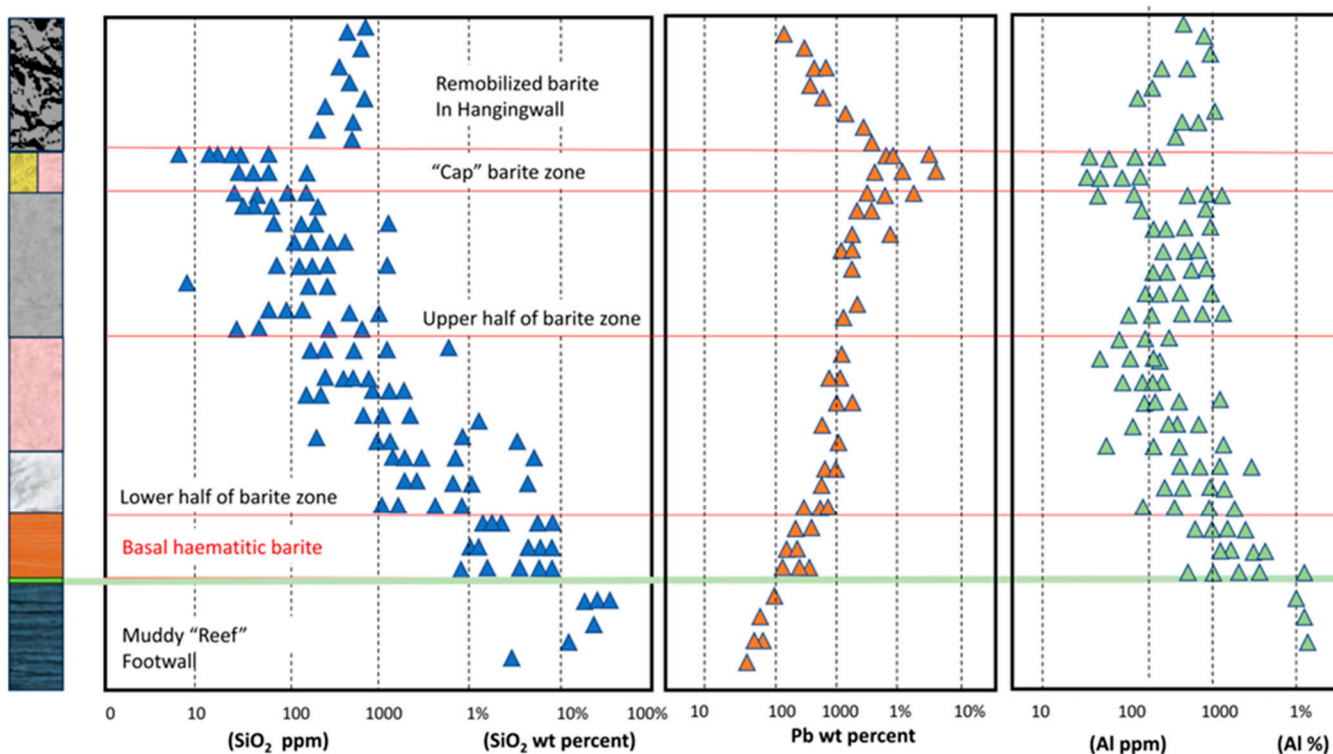


Figure 16. Geochemical profiles through the barite orebody in Ballynoe for analytical results for silica, lead, and aluminium. Redrawn from data from Barrett [13].

The wallrock geochemistry at Ballynoe and shows that the dispersion of anomalous Ba, Mn, Pb, and Zn values is strictly confined to the mineralised horizon directly overlying the Muddy Reef Limestone. Fe and SiO₂ reveal the only major association with the initial emplacement of the barite [13] with Ba and Fe appearing to have been co-precipitated from an aqueous solution in the presence of amorphous silicon in a semi-restricted marine lagoon. The subaqueous precipitation of barite is supported by sulphur and oxygen isotope data which suggests that contemporaneous seawater sulphate played a significant role in the deposition of the barite. In the more restricted areas of the lagoon (cut off by carbonate

mudbanks), lower Eh and pH conditions led to the precipitation of iron as siderite and/or pyrite. In such conditions the Ba would likely have remained in solution.

5.2. Biota in the Barite Orebody

There is significant evidence for contemporaneous environmental impact of the onset of the mineralising process towards the top of the Muddy Reef succession. The diameters of individual crinoid ossicles tend to increase in size until an abrupt extinction of the crinoid population occurs and crinoids are absent from the topmost 0.1 m [13,17]. A plot of the ossicle enlargement trend is shown in Figure 17. This size increase of the crinoids seen within the stratigraphy may be a direct consequence of changing physiochemical environments during sedimentation, the crinoids reflecting these conditions until for some reason mass extinction occurred. The crinoidal lenses may also exhibit severe slumping. A similar phenomenon is seen within a single bed of the uppermost Muddy Reef in the B-Zone where the crinoid ossicle size gradually increases laterally towards the chertification whereupon the crinoids cease to be found before passing laterally into grey and black non-fossiliferous cherts locally with distorted laminated pale sphalerite (Figures 11 and 15a). On the fringes of the chert development, crinoid ossicles show partial or total replacement by silica [13]. These two factors strongly suggest that towards the uppermost Muddy Reef and the diastem to the breccia sequence, a change in the physiochemistry of the depositional environment had an impact on the nature of the crinoid population.

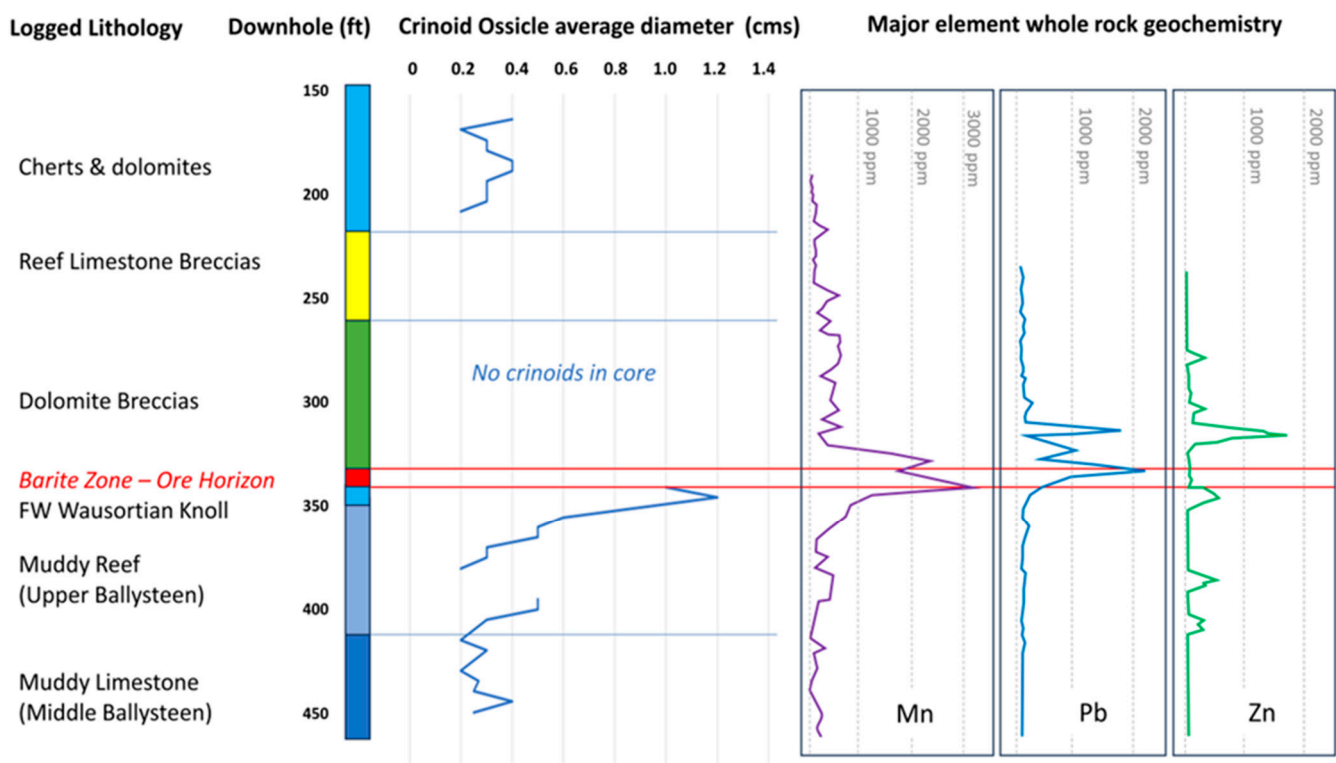


Figure 17. Plot of average crinoid ossicle diameters showing the notable increase towards the top of the Muddy Reef Limestone (Ballysteen Fm.). Also shown geochemical profiles for Mn, Pb, and Zn. Drawn from data in [13].

Barrett [13] noted that in the massive sulphides of Unit 6 in the barite orebody, the pyrite may develop tube-like structures which are up to 10 cm long by 1 cm in diameter, which he considered to resemble pyritised crinoid stems. These are now considered more likely to be worm casts and hydrothermal chimneys as described by Larter et al. [20] and Boyce et al. [6,7].

Larter et al. [20] identified the occurrence of fossil hydrothermal vents and a highly pyritic vent field in the south-western part of the Ballynoe pit at Silvermines. These fossil polychaete worms, which occur in pyritic mounds, have affinities to *Paravinella*, an organism that lives attached to hydrothermal chimneys at the Juan de Fuca hot spring site in the Northeast Pacific [40,41]. Stratiform beds of iron oxides (usually haematite) and silica—'jaspers'—are commonly associated with sulphide deposits in volcanic rock sequences in the geological record and are usually considered to be the product of low-temperature, diffuse hydrothermal venting, because of their close similarity to sea-floor mineral deposits at modern vent sites and on seamounts [42–44]. Such tubes of haematite cemented by silica, are similar to iron oxidising bacteria such as *Gallionella* which are typical of both fossil and modern submarine vent sites. The Ballynoe specimens of finely annulated pyritised tube worms share features in common with small alvinellid polychaetes observed in the Devonian Sibay and Cretaceous Bayda vent assemblages [44–46].

Additionally, the presence of pyrite microbialites and the presence of sub-micron, filamentous hollow tubes of haematite cemented by quartz suggest fossil iron-oxidising bacteria, which could indicate the existence of a chemoautotrophic, near-sea-floor habitat typical of both fossil and modern sea-floor hydrothermal systems. The interpreted presence of fossil vent-related worm tubes suggests that sea-floor exhalative hydrothermal activity could have occurred at Silvermines and Tynagh around 350–360 Ma [7,8,20,42,47].

Filamentous haematite microfossils in Ballynoe (Silvermines) jasper have also been described [47] showing a strong similarity to Fe-oxidising bacteria and provide evidence of microbial activity, a feature typical of modern and ancient vent fields [7]. Such filaments, identified as fossilised microbial communities [47,48] are mainly twisted hollow tubular structures and some are filled with later silica and typically are 1–20 µm in diameter and up to 200 µm long and are coated by sub-micron scale haematite crystals. All of the filaments are cemented by later silica phases, which can be either quartz or chalcedony. The fact that filaments often cross quartz and chalcedony crystal boundaries proves that the silica post-dates haematite filament formation [48]. Kucha [47] also noted the presence of sub-micron, filamentous hollow tubes of haematite cemented by quartz which he interpreted to be fossil iron-oxidising bacteria, supporting the existence of a near-sea-floor depositional environment.

Fossil evidence of the presence of a vent-related worm tube provides compelling evidence that sea-floor exhalative hydrothermal activity did occur at Silvermines and Tynagh. This implies that at least some of the mineralisation occurred contemporaneously with deposition of the carbonate host rocks during the Ivorian Stage, about 348 Ma [6]. The worm tubes are remarkably similar to examples described from modern volcanic-hosted massive sulphide deposits and fossilised examples from around ancient ones, and the filamentous microfossils have similarities to modern Fe-oxidising bacteria. There is no correlation between the worm tubes and normal Ivorian fossil assemblages such as crinoids, whose replacement by pyrite in the immediately underlying Ballynoe footwall is seen to destroy the original morphology. Convincingly, the sulphur isotope composition of the worm tube and host pyrite is essentially identical to that of the vent field pyrite and the main sulphide ore stage of Silvermines sulphides, all having a mean value of about −20‰, indicating an open-system bacteriogenic sulphide source.

6. Fluid Inclusions

Mullane & Kinnaird [17] in their study on Ballynoe barite reported that two-phase liquid-vapour inclusions ('L + V') are very irregular in shape. L + V inclusions lack solid phases and have a wide range of homogenisation temperatures, from 68 to 223 °C, with two peaks—one at 70–80 °C and the other at 190–200 °C (Figure 18). Salinities are in the range 9–25 equiv. wt% NaCl, again with two peaks—one at 10–11 equiv. wt% and the other at 23–24 equiv. wt% NaCl. In general, low-temperature inclusions are very saline (20%–25%) and higher-temperature inclusions are more dilute (9%–12%). There is a distinct break in sequence between these two fluid end-members, implying that there were two

fluids, one of moderate temperature and low salinity and the other of low temperature and high salinity. Low-temperature, high-salinity inclusions were present in all the units sampled, including one from a late-stage barite vein. The low-temperature, high-salinity inclusions display a general increase in homogenisation temperature from 68 to 110 °C between barite in Unit I and the crystalline cap barite in Unit 5. The moderate-temperature, low-salinity inclusions exhibit a similar pattern, from 150 °C to 220 °C (Figure 18).

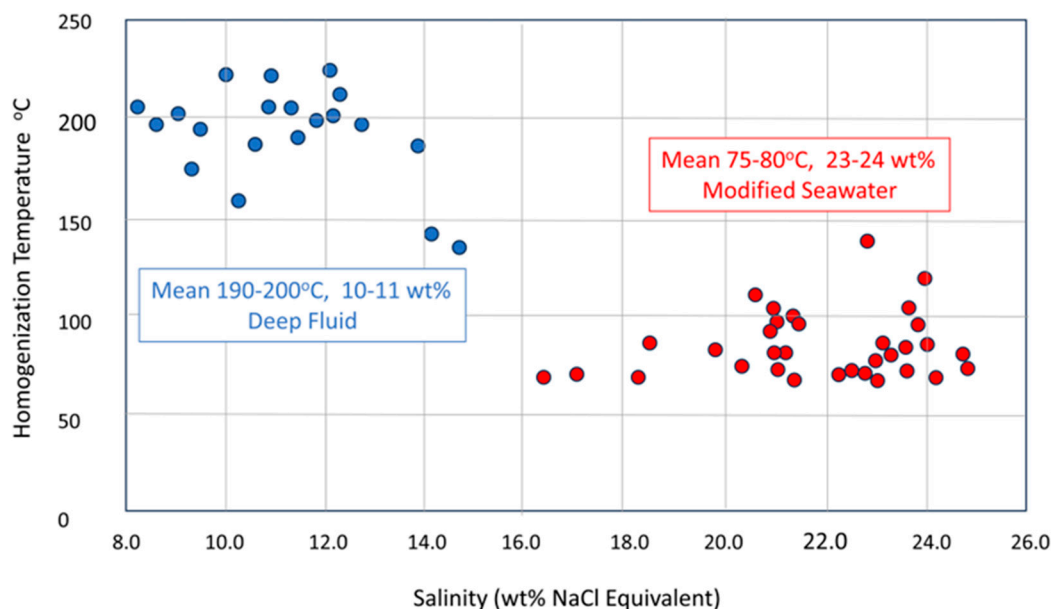


Figure 18. Fluid inclusion data from Ballynoe barite samples. Redrawn from data in [17].

Samson & Russell [49] in their study of the Silvermines sulphide orebodies record that fluid inclusion salinities range from 8 to 28 equiv. wt% NaCl with modes at 14 and 19 wt% NaCl. Leachate studies show the fluids to have high sodium concentration with lesser variable amounts of potassium and calcium and uniformly low magnesium concentrations ($K/Na = 0.03\text{--}0.23$; $Ca/Na = 0.03\text{--}0.28$; $Mg/Ca = 0.1\text{--}0.67$).

Homogenisation temperatures range from 50 ° to 260 °C, with most between 140° and 220 °C with a mode at 190 °C and a subsidiary group around 140 °C. Samson & Russell [49] suggest that the required pressure corrections are less than 5 °C, thus if the pressure within the epigenetic ore zones (Lower G and K-Zones) was purely hydrostatic, as is reasonable, a minimum seawater depth of around 80 m is required to prevent boiling of such fluids.

Samson & Russell [49] record those fluid inclusions in stellate crystal aggregates of diagenetic barite from the stratiform Ballynoe orebody which would seem to have grown in unconsolidated mud, close to the sea-floor [6], also have high salinities. This supports a model in which the upper parts of the system contained high-salinity fluids and further suggests that a brine pool existed on the sea floor during mineralisation.

7. Strontium Content and Isotopic Ratios

Barrett [13] reported that the barite from Ballynoe has a remarkably consistent content of strontium ranging from 1.96% $SrSO_4$ wt% in the basal haematitic barite to 2.45% wt% in the main orebody for a statistical average content of 2.33% $SrSO_4$ wt% ($n = 105$). The apparent lower value of $SrSO_4$ in the basal haematitic barite may be explained by the high SiO_2 and Fe_3O_4 content of the ore (up to 15% plus combined) which correspondingly reduces the $BaSO_4$ content and thus proportionally the $SrSO_4$ content.

The Sr isotope record of Dinantian seawater is characterised by a decline in the $^{87}Sr/^{86}Sr$ ratio from 0.7082 at the Devonian/Carboniferous transition from a high of 0.7080 in the early Hastarian to a low of 0.70765 in the late and mid-Chadian, with an early Chadian maximum at 0.7079 [50,51]. Superimposed on this trend are higher-order fluctuations with

a periodicity in the Ma range. The Dinantian seawater curve may potentially serve as a geochronological and correlation tool, particularly for the Hastarian to lower Chadian interval, where the attainable resolution is ~1 Ma [49,50]. Snoeck et al. [52] provide extensive Sr isotope data over the island of Ireland showing that the Lower Carboniferous succession in the Irish Midlands all fall within a range of $^{87}\text{Sr}/^{86}\text{Sr}$ equal to 0.7080 to 0.7090.

Sr isotope data indicate that strontium in the Ballynoe barite predominantly has an $^{87}\text{Sr}/^{86}\text{Sr}$ ratio of 0.7079 [52] indistinguishable from that demonstrated for Ivorian and early Chadian (Lower Carboniferous) sea water between 350–349 Ma and 345–344 Ma, respectively [50,53,54] (Figure 19).

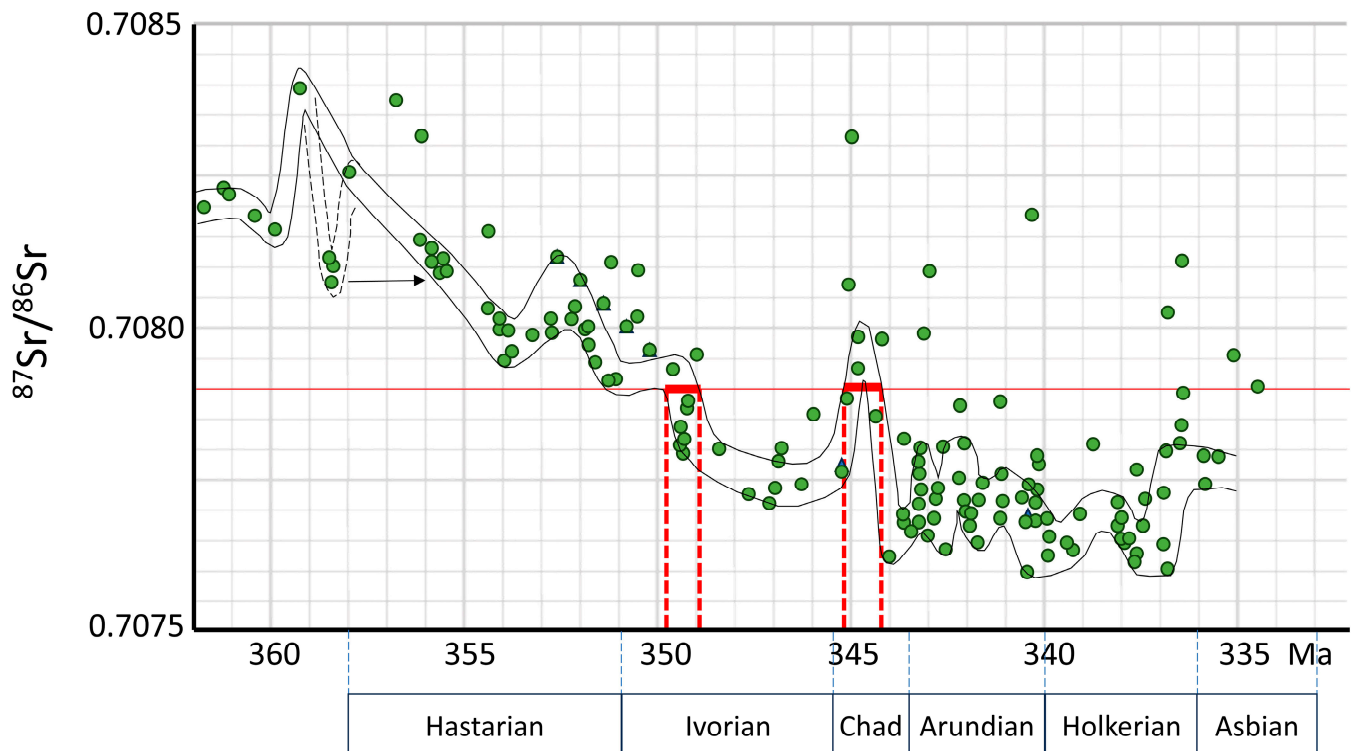


Figure 19. $^{87}\text{Sr}/^{86}\text{Sr}$ ratios of Ballynoe barite plotted on the LOWESS statistical regression function (*LOcally WEighted Scatterplot*) of Strontium Isotope Stratigraphy through the Lower Carboniferous Note correlation of Sr ratios of Ballynoe barites with ranges in the Ivorian and Chadian Stages identified by the red-dotted lines. Redrawn from [50,54].

8. Stable Isotopes of Hydrogen, Oxygen, and Sulphur

Fluid inclusion waters have δD values of -24 to -49‰ for quartz, -23 to -29‰ for dolomite-, -41 to -55‰ for barite, 28.9 to 54.7‰ for sphalerite, and -33 to -58‰ for galena. The $\delta^{18}\text{O}$ values of the mineralising fluids, calculated from mineral values, range from $+1.1$ to $+7.7\text{‰}$ for quartz and $+1.8$ to $+5.7\text{‰}$ for dolomite [49].

Oxygen isotope analyses of black chert from the immediate footwall to the barite in the Ballynoe open pit show little isotopic variation ($+25$ to $+27\text{‰}$), which is consistent with a diagenetic origin for the cherts in equilibrium with a fluid similar to Lower Carboniferous sea water at temperatures around 60 – 70 °C [19].

Isotopic values for the main orebody barite (Units 1 to 4) of $\delta^{18}\text{O}$ all fall in the range of $+13.0$ to $+14.5\text{‰}$ which is well within the range for Lower Carboniferous seawater. The minor variance from orebody isotopic values obtained from samples of secondary white ‘cap’ barite of Unit 5 with the isotope values for $\delta^{18}\text{O}$ $+17.5\text{‰}$ could suggest a later involvement of a more saline/evaporitic fluid [19] (Figure 20).

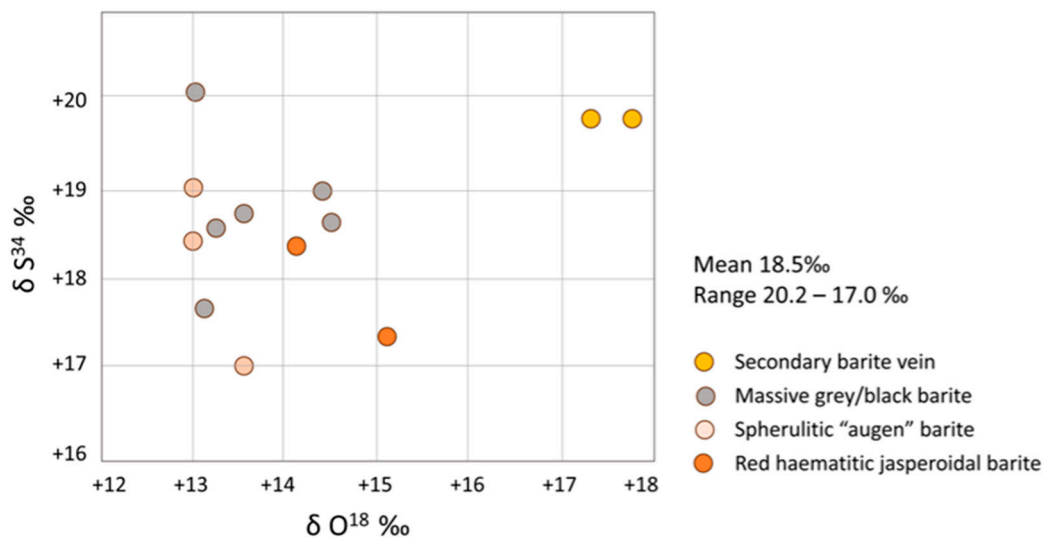


Figure 20. Sulphur isotopes and $\delta^{18}\text{O}$ values obtained for Ballynoe barite. Redrawn from data in [19].

The isotopic values for the orebody barite are clustered in the range $\delta^{34}\text{S}$ +18.6 to +19.0‰ [19]. Greig et al. [18] found that the barite at the distal end of the stratiform 'Upper G' zone and barite from the Ballynoe deposit had consistent isotope values around $\delta^{34}\text{S}$ +18.5‰, whilst Coomer & Robinson [19] report that for the orebody, barite $\delta^{34}\text{S}$ values are clustered in the range $\delta^{34}\text{S}$ +18.6 to +19‰, all consistent with direct derivation from Ivorian seawater sulphate [7,55–57].

The sulphur isotope signature ($\delta^{34}\text{S}$) from the base-metal stratiform orebodies (Upper G and B-Zones) is dominated by a signature about -20 ‰ indicative of an open-system bacteriogenic sulphide source, typical of Irish-type deposits [56]. The $\delta^{34}\text{S}$ values for the orebody barite fall within the range obtained for contemporaneous, Lower Carboniferous, seawater sulphate [55]. Figure 21 shows the range of seawater sulphate $\delta^{34}\text{S}$ values through the Lower Carboniferous and the extent of the ranges obtained from Ballynoe barites showing a coincidence between 354 and 345 Ma in the upper Hastarian to Ivorian [57].

Isotopic analysis on pyrite containing the worm tube fossils return a $\delta^{34}\text{S}$ of -23.2 ‰; whereas pyrite from a small section of worm tube gave a value of -18.4 ‰ [6,7]. Both of these values fall within the range of the dominant bacteriogenic signature from the stratiform deposits [18,19]. Collomorph pyrite and marcasite from throughout the barite open pit but outside the vent site, although having an average value about -19 ‰, has a very broad isotopic range (-40.4 to $+6$ ‰). This large range contrasts to the worm tube-related pyrite and associated vent-type pyrite in chimneys, which has a very restricted range of -18 to -19 ‰ [7]. All the isotopic results place the Ballynoe barite firmly within the hydrothermal field interacting with contemporaneous seawater [58].

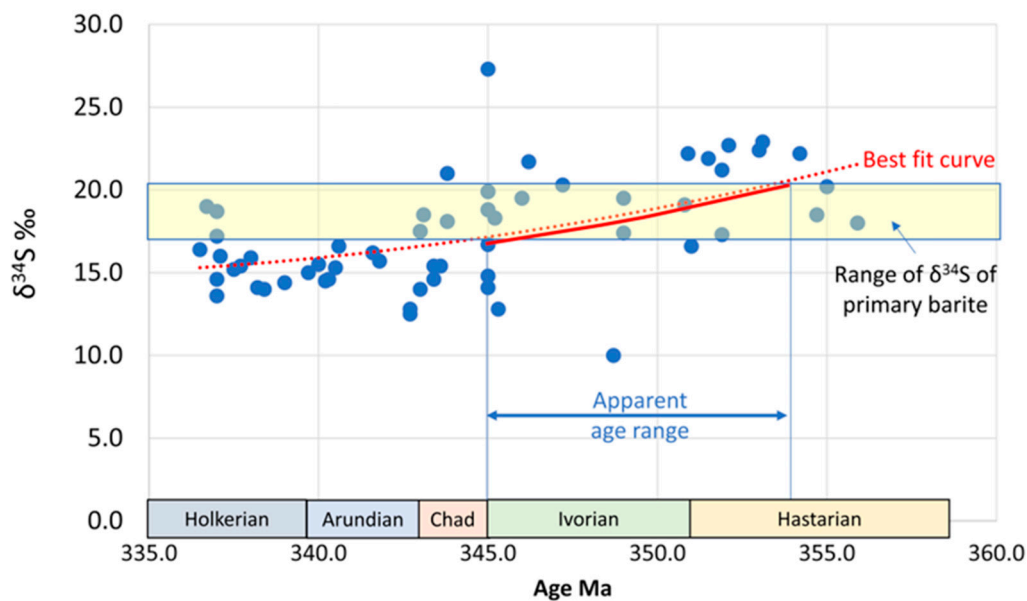


Figure 21. Diagram showing the range of seawater sulphate $\delta^{34}\text{S}$ values through the Lower Carboniferous and the extent of the ranges obtained from Ballynoe barites. Redrawn from data in [57].

9. Hangingwall Breccias

The hangingwall sequence to the tabular stratiform barite body comprises a sequence of well-bedded biomicrites and dolomite breccias. In the lower half of the succession the limestone has been dolomitised and heavily brecciated. This brecciation was initially interpreted to be the product of soft sediment slumping, and debris flow, probably induced by gentle movements along the Silvermines Fault zone (Figure 22) [33]. The breccias are extremely variable in lateral extent and horizons of brecciation intercalate with massive dolomites and Waulsortian mudbank limestones and show multiple well-developed slump planes, multiple brecciation, and graded bedding of the breccia clasts. Subsequent authors intimately familiar with the geology of the Silvermines district reiterated the interpretation of debris flows and in situ brecciation of soft sediments [2,6,7,13–16,20,39,59]. Whilst the breccias do have certain similarities to evaporite dissolution collapse breccias, there is no evidence for evaporites being present in time equivalent sequences in this part of the Irish Midlands.

Mullane & Kinnaird [17] described sedimentary cycles within the hangingwall breccia sequence, which is up to 32 m thick in the Ballynoe pit, with flow boundaries being well defined due to the presence of basal slip planes separating three distinct lithofacies: (1) a basal debris flow breccia, with bioclasts at the base, overlain by (2) dark banded limestones and (3) bioclastic breccias.

These debris-flow deposits, typically around 1 m in thickness, are pale-grey, poorly bedded, poorly sorted, and matrix-supported debris-flow deposits, with angular, sometimes imbricated clasts ranging in size from 0.03 to 0.30 m. The clasts are mainly of calcite but there are some of low-iron dolomite. In situ brecciation of the clasts is common, ranging from a single fracture to intense brecciation. The breccias are separated by thin, subordinate, impersistent horizons of bioclastic breccia, typically 20 cm thick, and minor lenses of banded limestone.

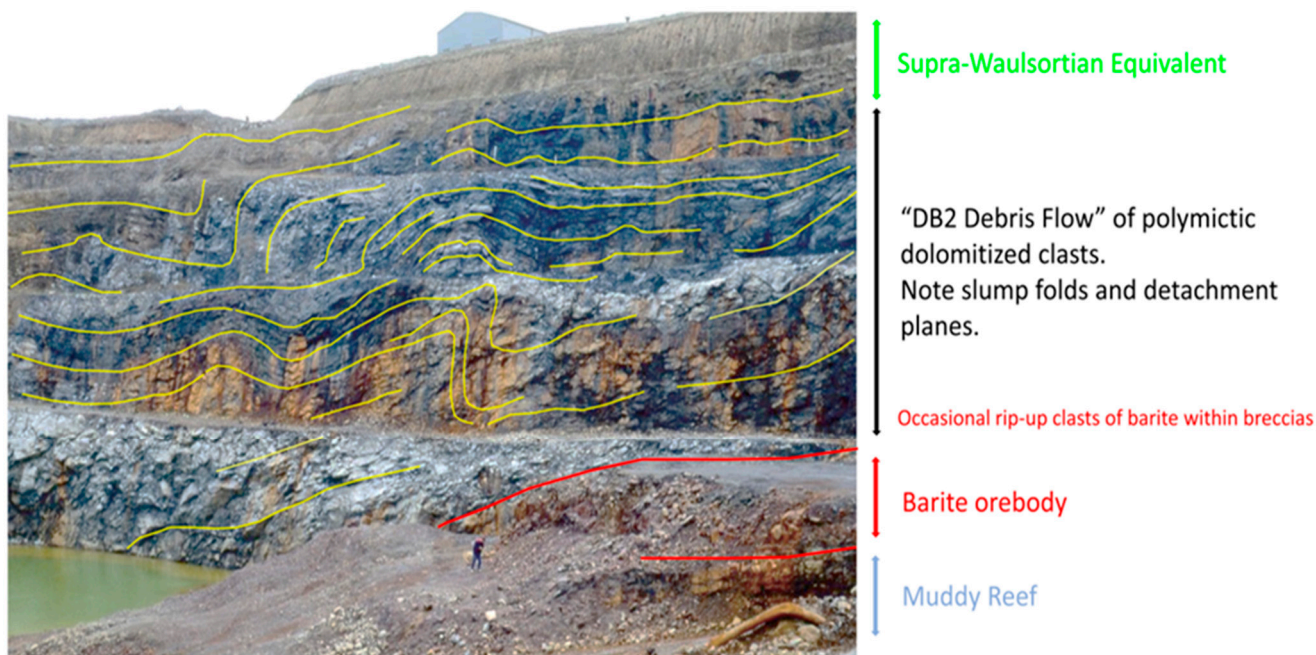


Figure 22. Annotated photograph of the north wall of the Ballynoe (Magcobar) open pit showing the slumped bedding and detachment folding form lines (yellow) within the “DB2” debris flow sequence overlying the barite orebody, seen in the bottom right of the photo (red lines).

Lee & Wilkinson [39] described individual breccia units as varying in thickness from 1 to 10 m, commonly with gradational boundaries. Sub-horizontal alignment of clasts is very common, and normally graded intervals up to 0.5 m thick are occasionally observed. Clasts of reworked limestone breccias demonstrate that there were multiple brecciation events.

Barrett [13] noted a very distinctive and continuous horizon within the dolomite breccia comprising a 1.5–3.0 m thick unit of very thin, filamentous, dolomite laminae that he regarded as being “of a possible stromatolitic affinity” which probably equates to the crenulated carbonate laminae within the banded argillaceous limestones in the cyclic unit recognised by Mullane & Kinnaird [17] (Figure 23a,b).

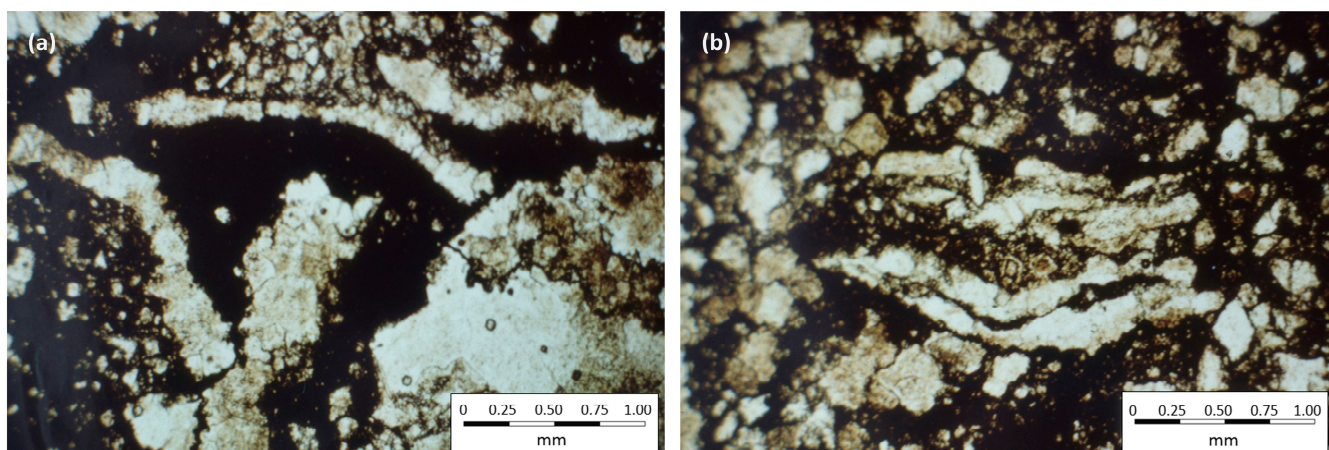


Figure 23. (a) Vermicular fabric of dolomite. Note the double growth direction from the central membrane of the organic material, curving from soft sediment compaction. ‘Upper G-Zone’ drillhole G-112, c. 38 m. (b) Elongated and wavy section of dolomite around an area of organic-rich carbonate mud. ‘B Zone’ drillhole B-190, c. 136 m.

Close to the basal contact of the breccia sequence with the underlying orebody, up to 15% of the clasts are angular and include angular rip-up clasts of lithified barite and flame or loading structures of pyrite into the base of the breccia sequence [2,13–17,33,39,58].

Isolated clasts of barite, colloform sphalerite, and laminated pyrite are commonly present in the lowest beds of the breccia sequence and can attain ore grade (>5% Zn + Pb) in the outer fringes of the Upper G and B-Zones (Figure 24b,c). These sulphide clasts range from rounded to angular and are typically 3 to 40 mm across with reworked clasts of banded sphalerite commonly showing evidence of dissolution during later (post-lithification?) dolomitisation, confirming that both phases did not precipitate from the same hydrothermal fluid [14,39].

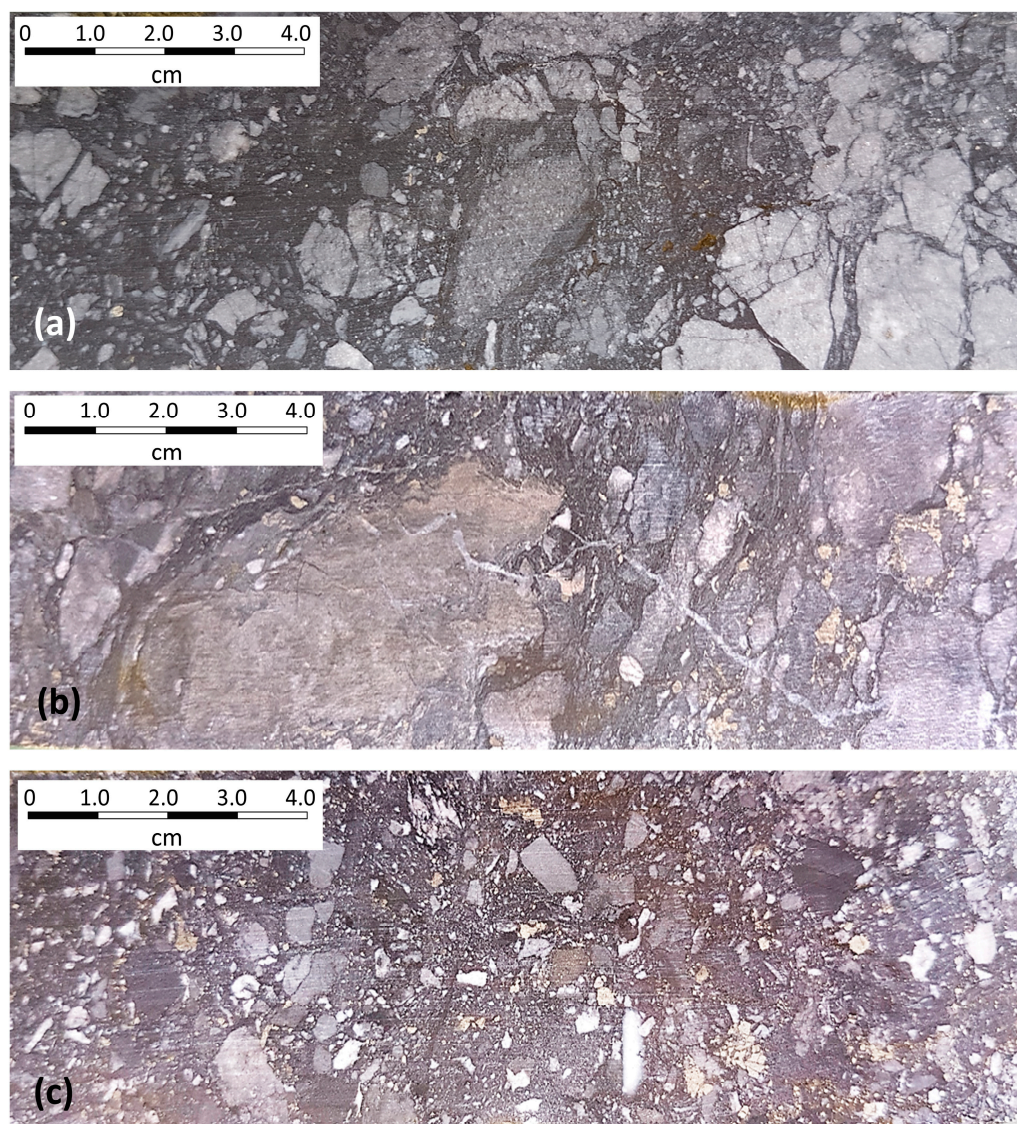


Figure 24. (a) Slightly pyritic Dolomite Breccia of dolomitised clasts set in a black dolomitic mud matrix. Note the mixture of jigsaw breccias and rounded coated clasts, ‘B Zone’ drillhole B-190, c. 138 m. (b) Limestone Breccia with small angular clasts of pyrite and a large, somewhat ragged clast with pale brown sphalerite mineralisation. Both the clasts and matrix are calcareous. ‘B-Zone’ drillhole B-56, c. 70.1 m. (c) Polymictic fine-grained debris-flow Dolomite Breccia with abundant angular clasts of pyrite. Upper G-Zone drillhole G-112, c. 96.1 m.

In clasts of Waulsortian-type mudbank limestones the stromatactis is mainly infilled with coarse subhedral calcite, but in the lower part of the geopetal infill is framboidal pyrite.

The orientation of the stromatolites within the clasts typically shows evidence of disturbance from its original depositional/crystallisation environment suggestive of mass tumbling chaotic flow [17].

In the upper half of the succession, the Dolomite Breccias tend to become more argillaceous and are increasingly replaced by a black or grey chert. In many instances, only the carbonaceous zones within the Dolomite Breccia are replaced, and examples are seen of angular, dolostone clasts being set in a matrix completely replaced by a black, homogeneous chert [13].

Dolomitisation of the hangingwall sequence is a distinctive feature of the rocks at Silvermines, with more than one generation of dolomite seen under cathodoluminescence in the breccias and mudbanks. Textures range from almost complete preservation of the original sedimentary features, through hazy recrystallisation, to almost total destruction of the original fabric leaving a saccharoidal and vuggy mosaic.

10. Discussion

Considerable controversy exists as to the timing of the important Lower Carboniferous carbonate-hosted Irish-type Zn + Pb +/- Ba +/- Ag deposits. The Silvermines stratiform ore zones including Ballynoe have been defined as an end member of this style in that in part they can be compellingly demonstrated to display textures indicative of on, or near, contemporaneous sea-floor deposition.

Among the strongest arguments in favour of this interpretation are the reports of a hydrothermal vent field including pyritic chimneys in the Ballynoe open-pit barite deposit [6,7,56] of delicately pyritised worm tubes hosted by massive pyrite and haematite filaments of apparent microbial origin [7]. These discoveries provide compelling evidence for the near-surface nature of parts of the Silvermines orebodies and imply that mineralisation had begun in the Irish Orefield by the late Hastarian age (around 350 Ma). This is consistent with interpretations of localised exhalative activity at Silvermines based on a range of geological and palaeontological features for at least part of the mineralising process [6,7,20,39]. In addition, a number of isotopic dating methods yield around similar ages [53].

The earliest manifestation of the mineralising processes is defined by the increasing influence of warm hydrothermal fluids accumulating in palaeotopographic lows influencing the size of crinoid ossicles and deposition of silica. Such palaeotopographic lows developing perpendicular to the principal fault trends indicate synsedimentary activity.

The onset of synsedimentary tectonism appears to be contemporaneous to early hydrothermal activity as is indicated by faunal flourishing and subsequent mass extinction towards the top of the Muddy Reef Limestone [13]. The increase in crinoid size and density apparently represents optimum conditions of nutrient and heat supply for growth followed by metal or sulphide toxicity. The Green Shale demarks a significant tectonostratigraphic diastem defining the onset of dynamic basin development and synsedimentary faulting. Immediately post-dating the Green Shale, the haematite, barite, and siderite appear to have been deposited coevally, and due to the tight palaeotopographic and stratigraphic control along with other evidence are most likely to have been formed at or just below the sediment/water interface.

In the B-Zone and parts of the Upper G-Zone, the barite/siderite is overlain by massive pyrite. This massive pyrite is strongly texturally zoned with coarse collomorph mounds developed close to the Silvermines Fault (in the case of the Upper G Zone) and the B Fault (in the case of the B Zone), immediately above either the haematite/barite or siderite or the Green Shale. Flanking these collomorph mounds is a fringe of coarse exfoliated colloform clasts which pass down the slope into progressively finer-grained laminated pyritic clastites and sulphidites. Above the massive pyrite, debris-flow dolomitic and limestone polymictic breccias contain angular rip-up clasts of pyrite and, locally, barite (Figures 15c and 24b,c).

Subsequent base-metal mineralisation appears to post-date the barium-iron facies with fine-grained galena and Schalenblende-type sphalerite infilling primary porosity (as

in the colloform pyrite) and replacing the argillaceous matrix in the polymictic breccias. Metal zoning shows lead and silver enriched close to the main faults and also becoming increasingly lead-rich up stratigraphy. Barrett [13] demonstrated that late crystalline barite (the 'cap' barite) formed by up dip migration of fluids post-main stage mineralisation.

Some contrarian opinions have suggested that the hangingwall breccias are collapse or dissolution features formed by hydrothermal activity with the barite and sulphides being deposited at the base of a giant cavity system. There are problems with such an interpretation including fundamental issues such as there being no evidence of fracturing penetrating supra-Waulsortian Equivalent (or indeed sub-Waulsortian) units as seen in the classical MVT-type deposits in Kildare [60,61].

Critically, at Silvermines there is no doubt that the breccias are thicker overlying the stratiform upper ore zones (Upper G-Zone and B-Zone). In these areas the breccias equivalent to the entire Waulsortian are thickened, clearly, contradicting a dissolution and collapse mechanism. The interpretation must surely be that the breccias are dominantly debris flows and this is supported by the presence of clasts of mineralisation included within the breccias, graded beds, rip-up and flame structures, and scouring. If they were formed by dissolution and collapse the sequence would, logically, have to be thinner over mineralisation as at, for example, Lisheen and Galmoy [62]. In addition, there is no evidence of a "roof" to sustain the collapse nor is there any subsidence of the supra-Waulsortian units which exhibit an undeformed layer-cake stratigraphy above a generally evenly dipping sedimentary interface. Such differences render an interpretation of dissolution and collapse difficult at best.

An additional important observation is that the footwall rocks at Silvermines are generally evenly bedded and maintain a uniform pattern until the very uppermost beds immediately below the Green Shale footwall to the upper orebodies. Hence, since both the underlying and overlying sequences to the breccias and to the mineralised horizon have a well-developed, tabular layer-cake disposition, with little if any thickness variation, this demonstrates clearly that the very variable thicknesses of the breccia sequence represent an anomalous time period in the sedimentary record.

11. Summary

Barrett [13], Andrew [2], and Mullane & Kinnaird [17] regarded the massive barite at Ballynoe (Silvermines) as being essentially sedimentary in origin and all described bedding features, slumping/debris flows and rip-up clasts as all having a primary sedimentary origin. Barrett [13] convincingly demonstrated that the wallrock geochemistry at Ballynoe suggests that the dispersion of anomalous Ba values is strictly confined to the mineralised horizon directly overlying the Muddy Reef Limestone and to the Footwall Waulsortian knolls. The stratiform nature of the Ba anomaly is still evident in areas well away from the effects of the main mineralisation. Iron and silicon were the only major elements which were associated with the initial emplacement of the barite.

A waning of the iron-rich phase heralded the bulk of the barite mineralisation which was initially very siliceous. The microspherulitic fabric of the barite suggests a rapid crystallisation. With the possible exception of minor (biogenic?) pyrite, the barite was free of accessory mineralisation possibly due to bottom water conditions being sufficiently oxidising to support a marine bottom fauna (at least episodically during barite precipitation) and would have been insufficiently reducing and sulphidic to induce efficient precipitation of metals. A gradual cessation of barite mineralisation witnessed the introduction of sphalerite and galena muds, which were the forerunners of the stratiform, sulphide cap to the orebody.

It is evident that the barite horizon has undergone considerable diagenetic modification since its original precipitation in the form of a cryptocrystalline mud, and the stylolitisation of the barite horizon must have been initiated during the early, relatively shallow compaction and lithification of the deposit. There is compelling evidence that the barite body must have lithified quickly, as angular rip-up clasts of barite, exhibiting identical features to that in the main orebody, are seen in the immediate hangingwall

breccias (Figure 15c) [2,14–17,39,58]. Similarly, Graham [33] described evidence of upward projecting tongues of pyrite into the breccias along the hangingwall contact of the 'Upper-G' zone massive pyrite body, which he attributed to the weight of the overlying debris flow sediments on the still plastic sulphides. Together this evidence strongly suggests that both the barite (siderite) and massive pyrite bodies were formed rapidly within the constraints of the palaeotopography and covered relatively quickly by flows of limestone and dolomitised limestone debris triggered by episodic movements on the Silvermines fault array.

Such features strongly suggest that the ore depositional environment was on or just below the contemporaneous sea-floor at around 348 Ma. This date agrees with various isotopic dates of between 350.5–348.2 Ma for the Green Shale [27], the $^{87}\text{Sr}/^{86}\text{Sr}$ ratio at between 350–349 Ma or 345–344 Ma and the $\delta^{34}\text{S}$ ‰ suggesting 354–345 Ma.

Thus, it is reasonable from the geological and isotopic evidence to conclude that the Ballynoe barite deposit formed by early local exhalation of ore-host facies (barite, siderite, pyrite) around 348 Ma marginally predating base-metal mineralisation which mainly occurred sub-sea-floor by void-fill and locally by replacement of carbonates during early diagenesis during shallow burial, during slumping and in situ (soft sediment) brecciation. The main depositional mechanism was by the mixing of high temperature metal-bearing brines with low temperature bacteriogenically active H_2S -rich modified seawater.

There is abundant evidence of tectonism contemporaneous to mineralisation and this is likely to have assisted in the rapid burial and early onset of diagenetic recrystallisation and stylolitisation of the barite at shallow burial depths. This, associated with the overall sag coincident with the extent of the mineralisation revealed from Connolly plots (Figures 9 and 10) clearly shows that contemporaneous tectonism was active at the time of the formation of the stratiform ore zones.

Recent U-Pb dating on a single unusual apatite crystal obtained from the hangingwall sequences spatially and geologically unrelated to the barite body at Ballynoe have returned ages of 331 ± 5.6 Ma [63], which correspond to the age of basin inversion in the Limerick–Clare areas immediately to the west [30].

The age of mineralisation is geologically and isotopically closely constrained and is contemporary with the Ivorian to late Chadian mineralisation elsewhere in the Irish orefield, ref. [1] predating the onset of basin collapse and late Chadian volcanism. Most workers support a model of formation at shallow depths typical of Irish-type deposits.

Ballynoe is part of the Silvermines district of the classic typomorph of Irish-type early syndiagenetic Zn–Pb–Ba–Ag ore deposits hosted in shallow water shelf limestones, which bear similarities to deposits in the Selwyn Basin and Kechika Trough in Western Canada (Anvil, Tom, Jason, Howards' Pass) and to parts of the giant Red Dog group of deposits in Alaska. Elsewhere in Europe, bedded barite is associated with sediment-hosted Pb–Zn deposits in Germany (Meggen and Rammelsberg) and Belgium (Chaudfontaine). The Cretaceous agreed Zn–Pb (\pm Ag \pm Ba) deposits in the Malayer-Esfahan Metallogenic belt of Iran have been described as Irish-type and have many features in common with Ballynoe (Silvermines) [64–66].

Funding: This research received no external funding.

Data Availability Statement: Data are contained within the article.

Acknowledgments: This paper is a personal review of the detailed observations and work of many earlier workers, notably John Barrett and Eta Mullane, whose detailed observations in the Ballynoe open pit during production operations are fundamental to our knowledge of the deposit, and to them I am grateful. I had the pleasure to work at Silvermines with Stuart Taylor, Eamonn Grennan, and the late George Emo at Magcobar, and although nearly 50 years ago now, I still recall their incisive comments and observations on the geology of these intriguing deposits. I would also like to thank the various reviewers of the initial drafts of this paper for their insights and evident improvements.

Conflicts of Interest: The author declares no conflict of interest.

Appendix A. Barite Elsewhere in the Irish Midlands Ore District and Surrounds (Figure 1)

In most of the Irish-type deposits in the Midlands, barite is difficult to quantify. Economically extracted barite at Ballynoe and Tynagh suggests that it is higher in the west of the orefield and, taken with Garrycam, suggests that the base of Waulsortian deposits may host higher levels of the mineral, although no significant levels of barite have been discovered along the Rathdowney Trend (Lisheen, Galmoy and Rapla) [62]. Perhaps notably, there is no discrete barite lens at Navan, by far the largest Irish-type deposit in the Midlands. However, barite is a common gangue in the Navan orebody, so the amount of barite is clearly significant, but is as yet unquantified [3].

At the Tynagh deposit (12.3 Mt @ 4.5% Zn, 4.6%Pb, 0.4% Cu, 52 g/t Ag), barite is a significant component of Stage 3 of the mineralising paragenesis occurring as veining and replacement of the host rocks and earlier ore textures by an assemblage dominated by tennantite, medium to coarsely crystalline galena, and coarse barite, and in certain bands comprises the major component. Milchem operated a retreatment plant on the Zn–Pb–Ag tailings recovering between 50,000 to 100,000 tpa for a total of 460,000 tonnes of barite from approximately 8.6 Mt of tailings, suggesting a content of around 5.3% barite in the Tynagh orebody.

The Keel Zn–Pb deposit occurs as disseminations and as stockwork sulphide mineralisation in Upper Devonian and Lower Carboniferous clastics and carbonates faulted against Lower Palaeozoic metasediments. Diamond drilling and underground exploration have outlined indicated and inferred resources of 1.85 Mt grading 7.71% Zn, 1.04% Pb, 0.12% Cd, and 39.6 g/t Ag. The Garrycam barite deposit is less than 1 km distant and is genetically related to the Keel mineralisation. The stratiform barite (with some sphalerite) is hosted in basal Waulsortian mudbank micrites. The deposit contains 1.35 Mt grading 2.67% Zn, 0.18% Pb, and 36.14% BaSO₄ [67].

Vein type deposits in County Cork at Clonakilty, Dereenalomane, and Derryginagh carry almost monomineralic white saccharoidal barite with traces of pyrite and specularite along fault zones up to 10 m in width over vertical depths in excess of 150 m.

The existence of barite at the Lady's Well barite mine near Clonakilty in County Cork was noted from the early 1800s with intermittent production around 1952 and again up until 1922. Milchem Ltd. reopened the mine in early 1979 following dewatering, and a 12-hole drilling programme completed in 1978 indicated a recoverable reserve of 230,000 t (to the –710 Level some 90 m below the lowest contemporary extant mine level) with a target annual production of 50,000 tpa. The deposit comprises an almost vertical E–W vein averaging 2 m in thickness, but locally up to 5 m thick. The barite is generally high grade (locally of chemical grade) and has been in production sporadically since 1855. Records show that approximately 5000 tpa had been produced from 1876 to 1901. More recently, 36,000 tpa had been produced between 1979 and 1985 initially by Milchem and later by NYM Limited to the –610 level.

The Derryginagh mine near Bantry, County Cork, was worked in the period 1864–1922 with mine workings extending over a strike length of 200 m and to a depth of 90 m. In the 1980s, four holes drilled by Dresser Minerals International Inc. intersected the barite vein over an average true width of 2.4 m at about 100 m below the surface and over a total strike length of 200 m. Further drilling by Sunrise Resources in 2012 led to the publishing of a scoping study for 278,340 tonnes of minable barite grading 67% BaSO₄ with further down-dip potential below 180 m, but nothing further ensued.

The Benbulbin (Glencarbury) mine in County Sligo, discovered in the latter part of the 19th century, a vertical vein of barite cuts the massive Lower Carboniferous limestones of Benbulbin Mountain, Co. Sligo. Averaging 1.2 m in thickness, the vein has been worked intermittently since 1875. Approximately 110,000 t of barite was produced between 1942 and 1960. More recently, approximately 10,000 tpa was produced between 1975 and 1979.

References

1. Andrew, C.J. Irish Zn-Pb deposits—A review of the evidence for the timing of mineralization. Constraints of stratigraphy and basin development. In *Irish-Type Deposits around the World*; Andrew, C.J., Hitzman, M.W., Stanley, G., Eds.; Irish Association for Economic Geology: Dublin, Ireland, 2023; pp. 169–210. [\[CrossRef\]](#)
2. Ashton, J.H.; Andrew, C.J.; Hitzman, M.W. Irish-type Zn-Pb deposits—What are they and more? In *Irish-Type Deposits around the World*; Andrew, C.J., Hitzman, M.W., Stanley, G., Eds.; Irish Association for Economic Geology: Dublin, Ireland, 2023; pp. 95–146. [\[CrossRef\]](#)
3. Andrew, C.J. The tectono-stratigraphic controls to mineralization in the Silvermines area, County Tipperary, Ireland. In *Geology and Genesis of Mineral Deposits in Ireland*; Andrew, C.J., Crowe, R.W.A., Finlay, S., Pennell, W.M., Pyne, J.F., Eds.; Irish Association for Economic Geology: Dublin, Ireland, 1986; pp. 377–418. [\[CrossRef\]](#)
4. Banks, D.A. Hydrothermal chimneys and fossil worms from the Tynagh Pb-Zn deposit, Ireland. In *Geology and Genesis of Mineral Deposits in Ireland*; Andrew, C.J., Crowe, R.W.A., Finlay, S., Pennell, W.M., Pyne, J.F., Eds.; Irish Association for Economic Geology: Dublin, Ireland, 1986; pp. 441–447.
5. Cruise, M.D. Iron Oxide and Associated Base-Metal Mineralization in the Central Midlands Basin, Ireland. Ph.D. Thesis, Trinity College, Dublin, Ireland, 2000.
6. Boyce, A.J.; Coleman, M.L.; Russell, M.J. Formation of fossil hydrothermal chimneys and mounds from Silvermines, Ireland. *Nature* **1983**, *306*, 545–550. [\[CrossRef\]](#)
7. Boyce, A.J.; Little, C.T.S.; Russell, M.J. A new fossil vent biota in the Ballynoe Barite deposit, Silvermines, Ireland: Evidence for intracratonic sea-floor hydrothermal activity about 352 Ma. *Econ. Geol.* **2003**, *98*, 649–656. [\[CrossRef\]](#)
8. Yesares, L.; Drummond, D.A.; Hollis, S.P.; Doran, A.L.; Menuge, J.F.; Boyce, A.J.; Blakeman, R.J.; Ashton, J.H. Coupling Mineralogy, Textures, Stable and Radiogenic Isotopes in Identifying Ore-Forming Processes in Irish-Type Carbonate-Hosted Zn-Pb Deposits. *Minerals* **2019**, *9*, 335. [\[CrossRef\]](#)
9. Yesares, L.; Menuge, J.F.; Blakeman, R.J.; Ashton, J.H.; Boyce, A.J.; David Coller, D.; Drummond, D.A.; Farrelly, I. Pyritic mineralization halo above the Tara Deep Zn-Pb deposit, Navan, Ireland: Evidence for sub-seafloor exhalative hydrothermal processes? *Ore Geol. Rev.* **2022**, *140*. [\[CrossRef\]](#)
10. Wynne, A.B. Memoir to accompany Sheet N° 154. *Mem. Geol. Sur. Irel.* **1861**, 1–52.
11. Griffith, S.V. *Mining Magazine: Serialized March 1955–January 1956*; The Silvermines Operation, Co.: Tipperary, Ireland, 1956.
12. Rhoden, H.N. Structure and economic mineralization of the Silvermines District, Co., Tipperary, Ireland. *Trans. Inst. Min. Metall.* **1958**, *68*, 67–94.
13. Barrett, J.R. Genesis of the Ballynoe Barite Deposit, Ireland and Other Stratabound Deposits of the United Kingdom. Unpub. Ph.D. Thesis, University of London, London, UK, 1975; 260p.
14. Taylor, S.; Andrew, C.J. Silvermines orebodies, Co. Tipperary, Ireland. *Trans. Inst. Min. Metall.* **1978**, *87*, B111–B124.
15. Taylor, S. Structural and palaeotopographic controls of lead-zinc mineralization in the Silvermines orebodies, Republic of Ireland. *Econ. Geol.* **1984**, *79*, 529–548. [\[CrossRef\]](#)
16. Andrew, C.J. The Silvermines District, Ireland. In *Irish Carbonate-Hosted Zn-Pb Deposits*; Guidebook Series; Anderson, I.K., Ashton, J.H., Earls, G., Hitzman, M.W., Tear, S., Eds.; Society of Economic Geologists: Littleton, ON, USA, 1995; Volume 21, pp. 247–258.
17. Mullane, M.M.; Kinnaird, J.A. Synsedimentary mineralization at Ballynoe barite deposit, near Silvermines, Co. Tipperary, Ireland. *Trans. Inst. Min. Metall.* **1998**, *107*, B48–B61.
18. Greig, J.A.; Baadsgard, H.; Cumming, G.L.; Folinsbee, R.E.; Krouse, H.R.; Ohmoto, H.; Sasaki, A.; Smejkal, V. Lead and sulfur isotopes of the Irish base metal mines in Carboniferous carbonate host rocks. In *Proceedings of the IMA-IAGOD Meetings '70, Joint Symposium Volume*; Society of Mining Geologists of Japan: Tokyo, Japan, 1971; pp. 84–92.
19. Coomer, P.G.; Robinson, B.W. Sulphur and sulphate—Oxygen isotopes and the origin of the Silvermines deposits, Ireland. *Miner. Depos.* **1976**, *11*, 155–169. [\[CrossRef\]](#)
20. Larter, R.C.L.; Boyce, A.J.; Russell, M.J. Hydrothermal pyrite chimneys from the Ballynoe barite deposit, Co. Tipperary, Ireland. *Miner. Depos.* **1981**, *16*, 309–318. [\[CrossRef\]](#)
21. Bruck, P.M. The regional lithostratigraphic setting of the Silvermines zinc-lead and the Ballynoe barite deposits, Co. Tipperary. In *Mineral Exploration in Ireland Progress and Developments 1971–1981*; Brown, A., Ed.; Irish Association for Economic Geology: Dublin, Ireland, 1982; pp. 162–170.
22. Grennan, E.F.; Andrew, C.J. The Mining Heritage and History of the Silvermines area, County Tipperary, Ireland since the 13th century. *Eur. Geol. J.* **2019**, *48*, 43–48.
23. Philcox, M. *Lower Carboniferous Lithostratigraphy of the Irish Midlands*; Irish Association for Economic Geology: Dublin, Ireland, 1984; 89p.
24. Lees, A. The structure and origin of the Waulsortian (Lower Carboniferous) ‘reefs’ of west-central Eire. *Philos. Trans. R. Soc. Lond. Ser. B* **1964**, *247*, 483–531.
25. Lees, A.; Miller, J. Facies variation in Waulsortian buildups, part 2; mid-Dinantian buildups from Europe and North America. *Geol. J.* **1985**, *20*, 159–180. [\[CrossRef\]](#)
26. Lees, A.; Miller, J. Waulsortian banks. In *Carbonate Mudmounds*; Monty, C.L.V., Bosence, D.W.J., Bridges, P.H., Pratt, B.R., Eds.; International Association of Sedimentologists Special Publication No. 23; Blackwell Science: Oxford, UK, 1995; pp. 191–271.

27. Phillips, W.E.A.; Sevastopulo, G.D. The stratigraphic and structural setting of Irish mineral deposits. In *Geology and Genesis of Mineral Deposits in Ireland*; Andrew, C.J., Crowe, R.W.A., Finlay, S., Pyne, J.F., Eds.; Irish Association of Economic Geologists: Dublin, Ireland, 1986; pp. 1–30.
28. Andrew, C.J. Mineralization in the Irish Midlands. In *Mineralization in the British Isles*; Chapman & Hall: London, UK, 1993; pp. 208–269.
29. Hitzman, M.W. Extensional faults that localize Irish syndiagenetic Zn-Pb deposits and their reactivation during Variscan Compression. In *Fractures, Fluid Flow and Mineralization*; McCaffrey, K.J.W., Lonergan, L., Wilkinson, J.J., Eds.; Special Publications; Geological Society: London, UK, 1999; Volume 155, pp. 233–245.
30. Strogon, P. The Carboniferous lithostratigraphy of Southeast County Limerick, Ireland, and the origin of the Shannon trough. *Geol. J.* **1988**, *23*, 121–137. [[CrossRef](#)]
31. Koch, H.A.; Chew, D.; Hitzman, M.; Slezak, P.; Dunleavy, E.; Holdstock, M. Age constraints of the mineralized Waulsortian limestone formation by dating of Irish volcanic ash layers. In Proceedings of the IAEG Conference “Getting Back to Business”, Athlone, Ireland, 21–22 May 2022.
32. Kyne, R.; Torremans, K.; Güven, J.; Doyle, R.; Walsh, J. 3-D Modelling of the Lisheen and Silvermines Deposits, County Tipperary, Ireland: Insights into Structural Controls on the Formation of Irish Zn-Pb Deposits. *Econ. Geol.* **2019**, *114*, 93–116. [[CrossRef](#)]
33. Graham, R.A. The Mogul Base-Metal Deposits, Co, Tipperary, Ireland, Unpub. Ph.D. Thesis, University of Ontario, Oshawa, ON, Canada, 1970; 227p.
34. Locklin, J.A. *Petrologic Analysis of Core Samples from the Silvermines Mineral District, Co. Tipperary*; Research Report; Getty Research Center: Los Angeles, CA, USA, 1983; 28p.
35. Schultz, R.W. Lower Carboniferous Cherty Ironstones at Tynagh, Ireland. *Econ. Geol.* **1966**, *61*, 311–342. [[CrossRef](#)]
36. Catlin, S. *Irish Base Metals Core Description: Mineralization in Core Samples from the Silvermines Area, Ireland*; Research Report; Getty Research Center: Los Angeles, CA, USA, 1983; pp. 83–325, 22p.
37. Gross, G.A. Primary features in cherty iron formations. *Sed. Geol.* **1972**, *7*, 241–261. [[CrossRef](#)]
38. Pratt, B.R. Syneresis cracks: Subaqueous shrinkage in argillaceous sediments caused by earthquake-induced dewatering. *Sediment. Geol.* **1998**, *117*, 1–10. [[CrossRef](#)]
39. Lee, M.J.; Wilkinson, J.J. Cementation, hydrothermal alteration and Zn-Pb mineralization of carbonate breccias in the Irish Midlands: Textural evidence from the Cooleen Zone, near Silvermines, Co. Tipperary. *Econ. Geol.* **2002**, *97*, 653–662. [[CrossRef](#)]
40. Rustichelli, A.; Tondi, E.; Korneva, I.; Baud, P.; Viniguerra, S.; Agista, F.; Reuche, T.; Janiseck, J.-M. Bedding-parallel stylolites in shallow-water limestone successions of the Apulian Carbonate Platform (central-southern Italy). *Ital. J. Geosci.* **2015**, *134*, 513–534. [[CrossRef](#)]
41. Desbruères, D.; Gaill, F.; Laubier, L.; Fouquet, Y. Polychaetous annelids from hydrothermal vent ecosystems: An overview. In *The hydrothermal Vents of the Eastern Pacific: An Overview*; Jones, M.L., Ed.; INFAX Corporation: Vienna, Virginia, 1985; pp. 103–116.
42. Russell, M.J. The generation at hot springs of sedimentary ore deposits, microbialites and life. *Ore Geol. Rev.* **1996**, *10*, 199–214. [[CrossRef](#)]
43. Juniper, S.K.; Fouquet, Y. Filamentous iron-silica deposits from modern and ancient hydrothermal sites. *Can. Miner.* **1988**, *26*, 859–869.
44. Peng, X.; Zhou, H.H.; Tang, S.; Yao, H.; Jiang, L.; Wu, Z. Early-stage mineralization of hydrothermal tubeworms: New insights into the role of microorganisms in the process of mineralization. *Chin. Sci. Bull.* **2008**, *53*, 251–261. [[CrossRef](#)]
45. Oudin, E.; Bouladon, J.; Paris, J.P. Vers hydrothermaux fossils dans une mineralisation sulfuree des ophiolites de Nouvelle-Calédonie. *Acad. Sci. C. R. Ser. II* **1985**, *301*, 157–162.
46. Kuznetsov, A.P.; Maslennikov, V.V.; Zaikov, V.V. The near-hydrothermal fauna of the Silurian paleo-ocean in the south Ural. *Izv. Akad. Nauk SSSR Ser. Biol.* **1993**, *4*, 525–534.
47. Kucha, H. Bacterially Induced: Micro- to Nano-Textures, Intermediate and Mixed Sulfur Valences, and S Isotopes of Massive Sulphides, Silvermines Zn-Pb Deposit, Ireland. 2017. Available online: https://www.researchgate.net/publication/325827752_Silvermines_Book (accessed on 20 January 2020).
48. Little, C.T.S.; Thorseth, I.H. Hydrothermal vent microbial communities: A fossil perspective. *Carb. Biol. Mar.* **2002**, *43*, 317–319.
49. Samson; Russell, M.J. Fluid inclusion data from the Silvermines lead-zinc-barite deposits, Ireland. *Trans. Inst. Min. Metall.* **1983**, *92*, 67–71.
50. Bruckschen, P.; Bruhn, F.; Veizer, J.; Buhl, D. ⁸⁷Sr/⁸⁶Sr isotopic evolution of Lower Carboniferous seawater: Dinantian of Western Europe. *Sediment. Geol.* **1995**, *100*, 63–81. [[CrossRef](#)]
51. Bruckschen, P.; Oesmann, S.; Veizer, J. Isotope stratigraphy of the European Carboniferous: Proxy signals for ocean chemistry, climate and tectonics. *Chem. Geol.* **1999**, *161*, 127–163. [[CrossRef](#)]
52. Snoeck, C.; Ryan, S.; Pouncett, J.; Pellegrini, M.; Claeys, P.; Wainwright, A.N.; Mattielli, N.; Lee-Thorp, J.A.; Schulting, R.J. Towards a biologically available strontium isotope baseline for Ireland. *Sci. Total Environ.* **2020**, *712*, 136248. [[CrossRef](#)] [[PubMed](#)]
53. Schneider, J.; von Quadt, A.; Wilkinson, J.J.; Boyce, A.J. Age of the Silvermines Irish-type Zn-Pb deposit from direct Rb-Sr dating of sphalerite. In *Digging Deeper: Proceedings of the Ninth Biennial SGA Meeting*; IEAG: Dublin, Ireland, 2007; pp. 373–376.
54. Chen, J.; Chen, B.; Montañez, I.P. Carboniferous isotope stratigraphy. *Geol. Soc. Lond. Spec. Publ.* **2020**, *512*, 197–211. [[CrossRef](#)]
55. Thode, A.G.; Monster, J. Sulphur isotope geochemistry of petroleum evaporites and ancient seas. *Fluids Subsurf. Environ.* **1965**, *4*, 367–377.

56. Fallick, A.E.; Ashton, J.H.; Boyce, A.J.; Ellam, R.M.; Russell, M.J. Bacteria were responsible for the magnitude of the world-class hydrothermal base-metal orebody at Navan, Ireland. *Econ. Geol.* **2001**, *96*, 885–890. [[CrossRef](#)]
57. Boyce, A.J.; Fallick, A.E.; Mullen, G.; Drummond, D.; Doran, A. Taking account of sulfur isotope geochemistry in the genesis of Irish-type base-metal deposits. In *Irish-Type Deposits around the World*; Irish Association for Economic Geology: Dublin, Ireland, 2023; Available online: <https://view.officeapps.live.com/op/view.aspx?src=https://iaeg.ie/resources/Documents/Boyce.pptx&wdOrigin=BROWSELINK> (accessed on 21 February 2024).
58. Griffith, E.M.; Paytan, A. Barite in the ocean—Occurrence, geochemistry and palaeoceanographic applications. *Sedimentology* **2012**, *59*, 1817–1835. [[CrossRef](#)]
59. Fillion, M. Economic Geology and Geostatistics of Base Metal Mineralisation at Silvermines, Ireland, Unpub. Ph.D. Thesis, University of London, London, UK, 1973; 360p.
60. Holdstock, M.P. Breccia-hosted Zinc-Lead mineralization in Tournaisian and Lower Visean Carbonates at Harberton Bridge, County Kildare. In *Mineral Exploration in Ireland: Progress and Developments 1971–1981*; Brown, A.G., Pyne, J.F., Eds.; Irish Association for Economic Geology: Dublin, Ireland, 1982; pp. 83–91.
61. Andrew, C.J.; Stanley, G. Irish, but not Irish-type. In *Irish-Type Deposits around the World*; Andrew, C.J., Hitzman, M.W., Stanley, G., Eds.; Irish Association for Economic Geology: Dublin, Ireland, 2023; pp. 211–230. [[CrossRef](#)]
62. Guven, J.; Torremans, K.; Johnson, S.; Hitzman, M. The Rathdowney Trend, Ireland: Geological evolution and controls on Zn-Pb mineralization. In *Irish-Type Deposits around the World*; Andrew, C.J., Hitzman, M.W., Stanley, G., Eds.; Irish Association for Economic Geology: Dublin, Ireland, 2023; pp. 329–362. [[CrossRef](#)]
63. Vafeas, N.; Slezak, P.; Chew, D.; Brodbeck, M.; Hitzman, M.; Hnatyshin, D. U-Pb dating of apatite from Silvermines deposit, Ireland: A model for hydrothermal ore genesis. *Econ. Geol.* **2023**, *118*, 1521–1527. [[CrossRef](#)]
64. Jewell, P.W. Bedded barite in the Geological Record. In *Marine Authigenesis: From Global to Microbial*; Glenn, C.R., Prévôt-Lucas, L., Lucas, J., Eds.; SEPM Society for Sedimentary Geology: Tulsa, Oklahoma, 2000. [[CrossRef](#)]
65. Mahmoodi, P.; Peter, J.M.; Rajabi, A.; Rastad, E. Geological and textural characteristics as evidence for Irish-type mineralization in the Eastern Haft-Savaran deposit. In *Irish-Type Deposits around the World*; Andrew, C.J., Hitzman, M.W., Stanley, G., Eds.; Irish Association for Economic Geology: Dublin, Ireland, 2023; pp. 533–544. [[CrossRef](#)]
66. Rajabi, A.; Mahmoodi, P.; Rastad, E.; Canet, C.; Alfonso, P.; Niroomand, S.; Tarmohammadi, A.; Perrnajmodin, H.; Akbari, Z. An introduction to Irish-type Zn-Pb deposits in early Cretaceous carbonate rocks of Iran. In *Irish-Type Deposits around the World*; Andrew, C.J., Hitzman, M.W., Stanley, G., Eds.; Irish Association for Economic Geology: Dublin, Ireland, 2023; pp. 511–532. [[CrossRef](#)]
67. Slowey, E.P. The Zn-Pb and barite deposits at Keel, County Longford. In *Geology and Genesis of Mineral Deposits in Ireland*; Andrew, C.J., Crowe, R.W.A., Finlay, S., Pennell, W.M., Pyne, J.F., Eds.; Irish Association for Economic Geology: Dublin, Ireland, 1986; pp. 319–330. [[CrossRef](#)]

Disclaimer/Publisher’s Note: The statements, opinions and data contained in all publications are solely those of the individual author(s) and contributor(s) and not of MDPI and/or the editor(s). MDPI and/or the editor(s) disclaim responsibility for any injury to people or property resulting from any ideas, methods, instructions or products referred to in the content.